Quantum transport in nanostructures

About the manifestations of quantum mechanics on the electrical transport properties of conductors

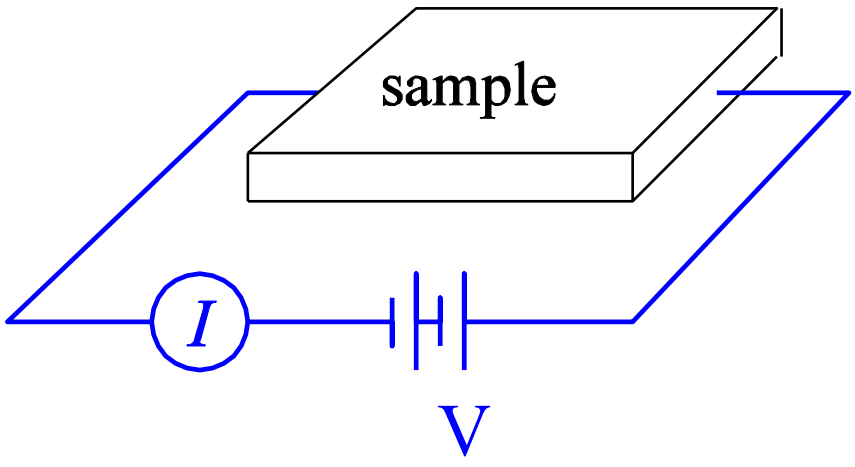

At macro scale

$I = V/R$ (Ohm's law)

$= \sigma V$

At nano scale

I ? V

Moore’ s Law

The number of transistors per microchip doubles roughly every three years.

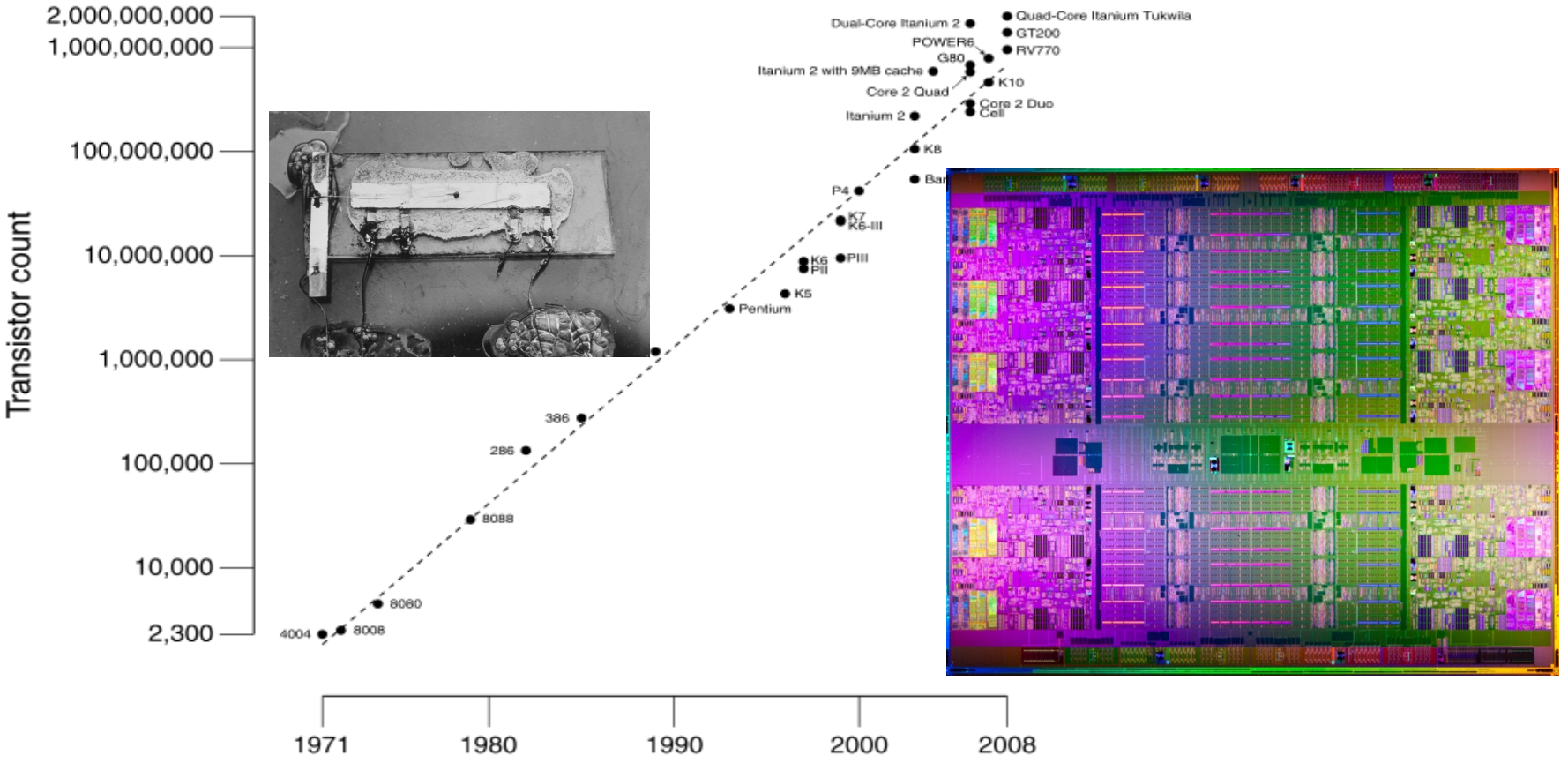

Nanoscale electronics

Nanotubes/wires

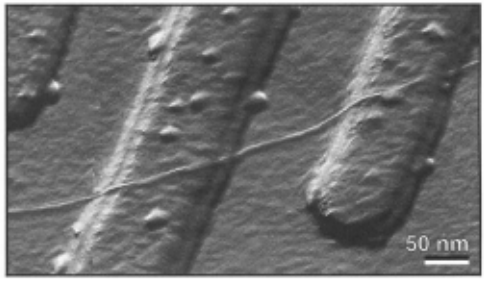

Tans *et al.* (1997)

Atomic point contacts

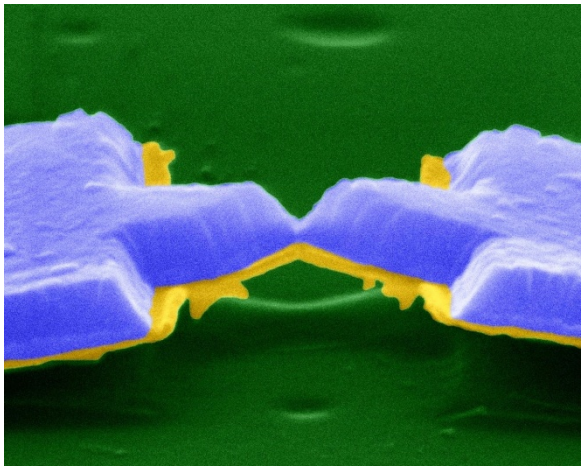

Scheer *et al.* (1998)

Molecular junctions

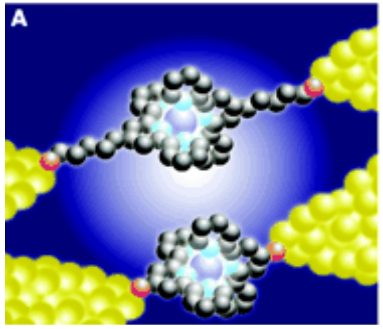

from Nitzan *et al.* (2003)

Organic electronics

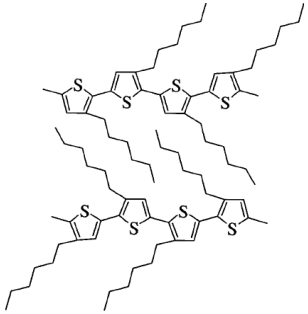

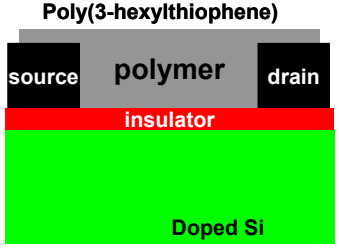

Z.Q. Li *et al.* (2006)

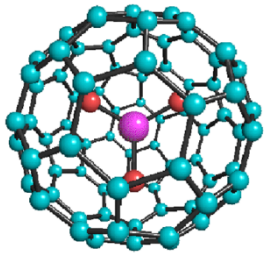

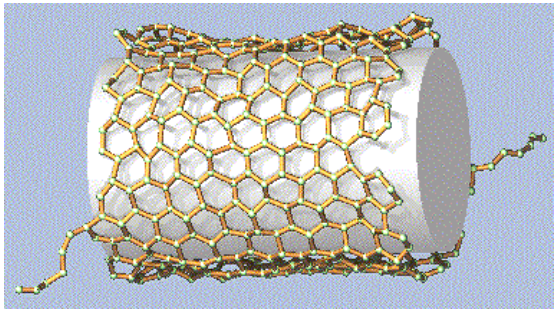

Fast DNA sequencing

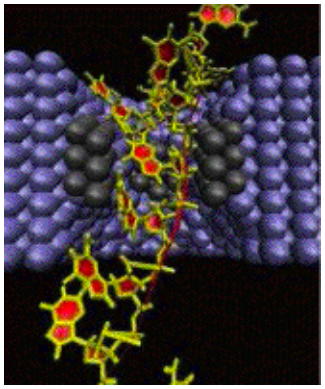

Lagerqvist *et al.* (2006)

Expected effects for electrons in nanostructures

- Quantum confinement effect
- Tunneling effects
- Charge discreteness and strong electron-electron Coulomb interaction effects
- Strong electric field effects
- Ballistic transport effects

Important mesoscopic regimes

conventional device: 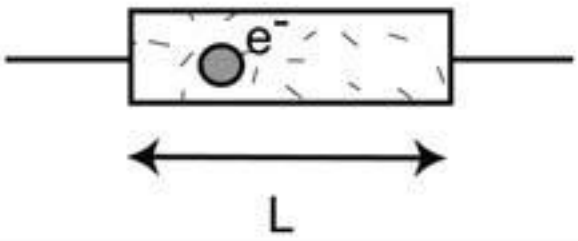		mesoscopic device: 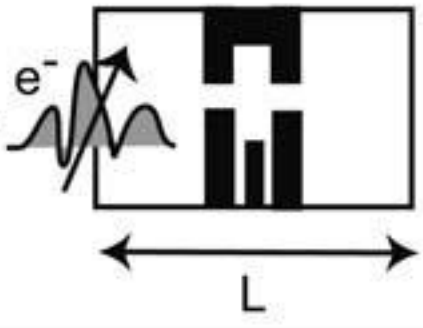	
$L \gg l_e$	diffusive	$L \lesssim l_e$	ballistic
$L \gg l_\phi$	incoherent	$L \lesssim l_\phi$	phase coherent
$L \gg \lambda_F$	no size quantization	$L \lesssim \lambda_F$	size quantization
$e^2/C < k_B\Theta$	no single electron charging	$e^2/C \gtrsim k_B\Theta$	single electron charging effects
$L \gg l_s$	no spin effects	$L \lesssim l_s$	spin effects

Important length scales

Elastic mean free path (l_e): average distance the electrons travel without being elastically scattered

$l_e = v_F \tau_e$. v_F denotes the Fermi velocity of the electrons

Phase coherent length (l_Φ): average distance the electrons travel before their phase is randomized

$l_\Phi = v_F \tau_\Phi$. τ_Φ denotes the dephasing time of the electrons

Fermi wavelength (λ_F): de Broglie wavelength of Fermi electrons

in d = 3: $\lambda_F = 2^{3/2}(\pi/3n)^{1/3}$

in d = 2: $\lambda_F = (2\pi/n)^{1/2}$

in d = 1: $\lambda_F = 4/n$

Quantum wires and point contact

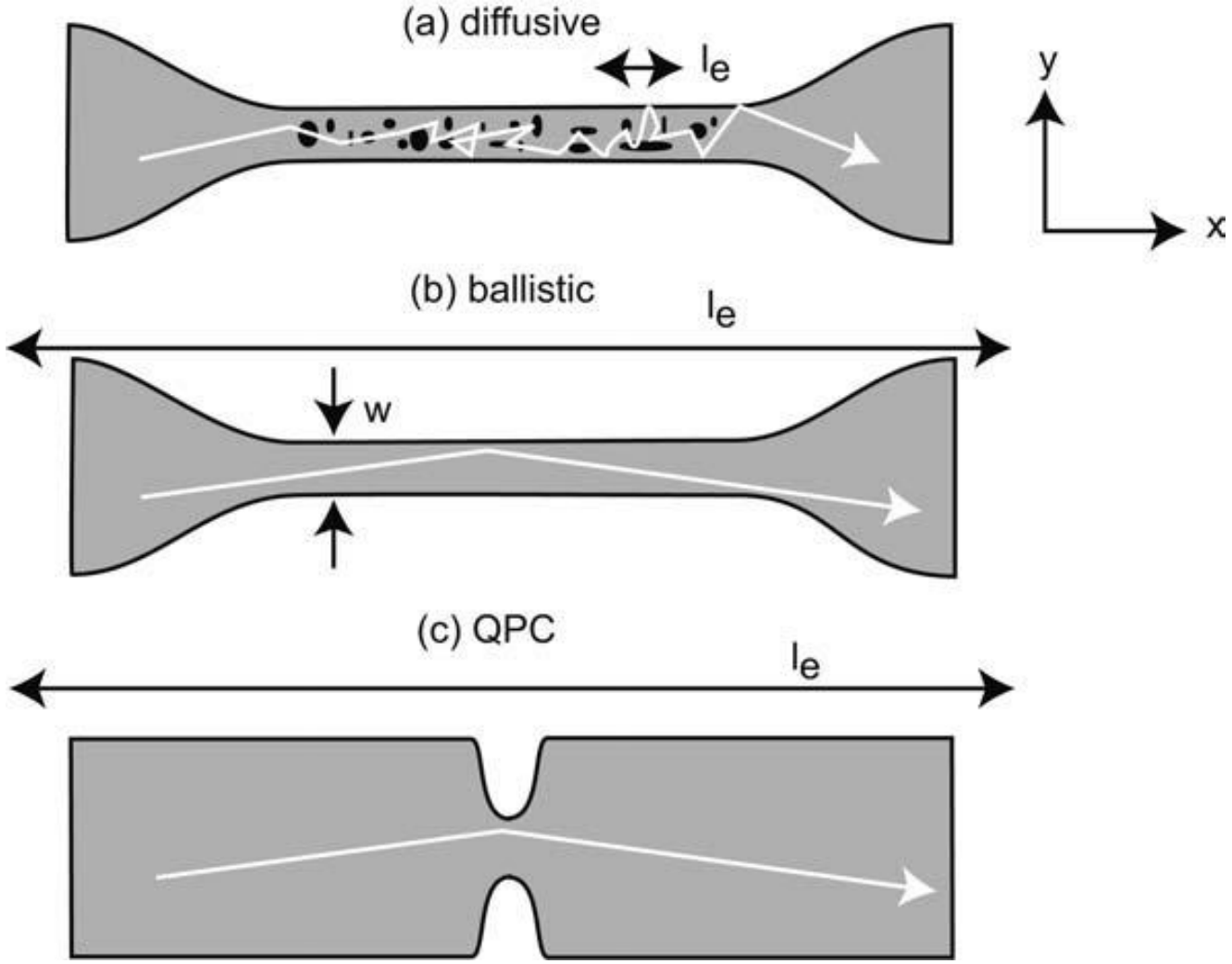

Typical length scale for mesoscopic regime

Temperature (K)	L* (nm)
4.2 (liquid helium)	< 5000
77 (liquid nitrogen)	< 100
300 (room temperature)	< 10

*The numbers just give an order of magnitude

Conduction at the macroscale

- Large number of states contribute to overall current
- Large number of electrons
- Resistivity, mobility, electric field, bias voltage, macrocopic currents are well-defined
- Quantum effects are averaged out by thermal effects

Conduction at the nanoscale

- Small number of states can affect the overall current
- Wavefunction coherence lengths are comparable to characteristic device dimensions
- Single electrons charging effects can be significant
- These can amount to overall macroscopic electronic properties that show deviations from bulk electronic properties

Bolztmann Transport Equation

Based on the semiclassical transport theory, considering the distributions of carriers to energies and momenta, taking into account scatterings.

The electrons obey the semiclassical equations of motion

$\mathbf{v}(\mathbf{k}) = (1/\hbar)\nabla_k \varepsilon(\mathbf{k})$

$d\mathbf{k}/dt = -e/\hbar\,(\mathbf{E} + \mathbf{v}(\mathbf{k}) \times \mathbf{B})$

The general Boltzmann equation to first order approximation:

$\mathbf{v}(\mathbf{k}) \bullet \nabla\varphi(\mathbf{k},\mathbf{r},t) - e\mathbf{E}/\hbar \bullet \nabla_k \varphi(\mathbf{k},\mathbf{r},t) + \partial\varphi(\mathbf{k},\mathbf{r},t)/\partial t = [\partial\varphi(\mathbf{k},\mathbf{r},t)/\partial t]_{scatter}$

Current density equals to the conductance times electric field

$j = \sigma E$

With simplified Bolztmann equation

$\sigma = ne^2 \tau_D/m^* = ne\,\mu$

the electron mobility $\mu \equiv e\,\tau_D/m^*$.

Flow of electrons between two reservoirs

Electrons obey the Fermi-Dirac distribution

A metal/semiconductor electrode

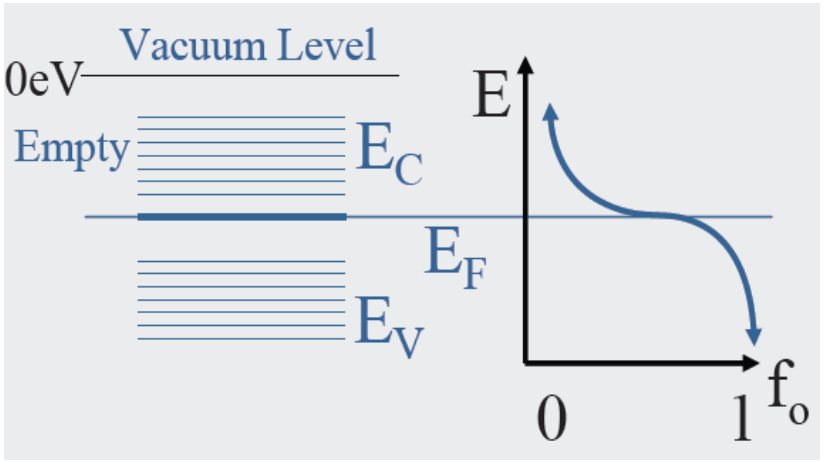

As T ~ 0 K, this is a step function

Two electrodes with some other material (states) in between

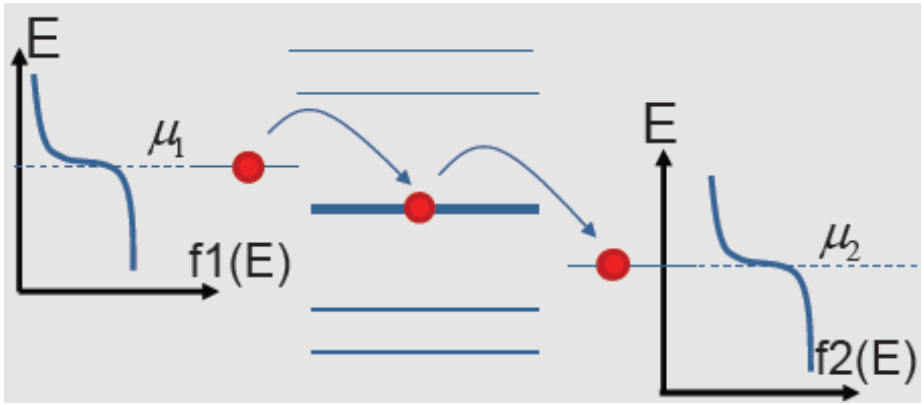

Availability of carriers on the left, and empty slots on the right, how fast the carriers tunnel from the left to the center and how fast the carriers tunnel from the center to the right basically determine the current.

Molecular Break Junctions

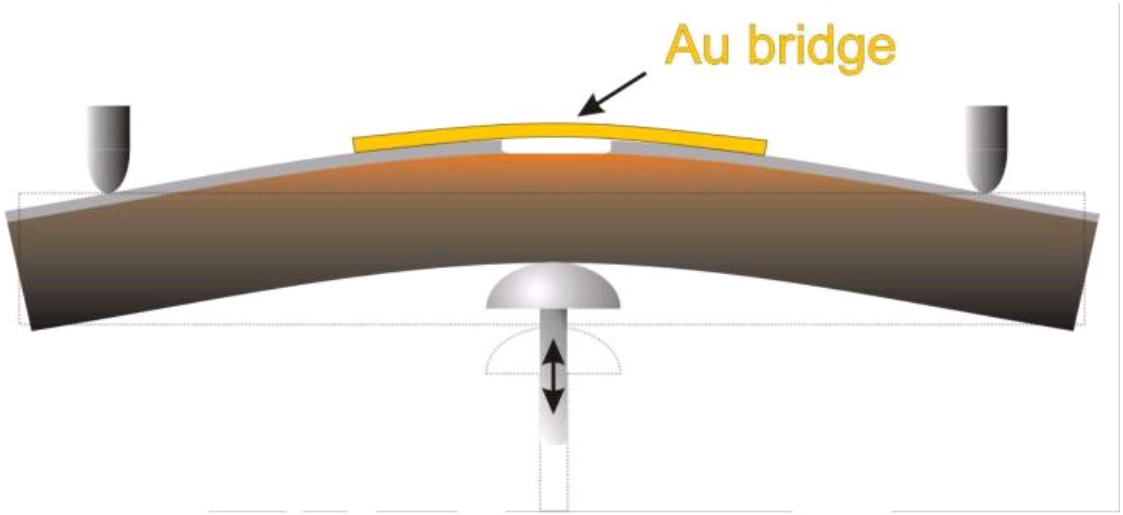

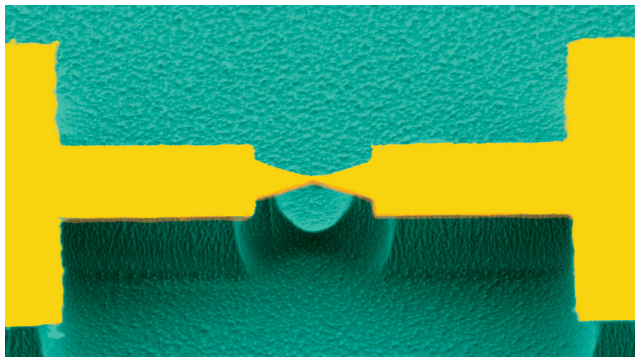

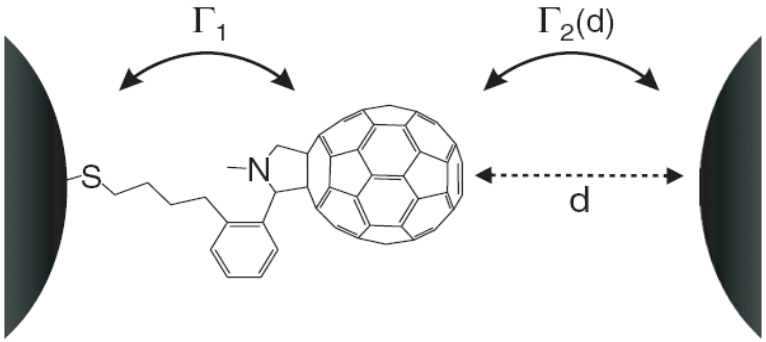

Figure 1. Schematic representation of a break junction with a thiolated C_{60} molecule anchored to the left electrode. The distance *d* between the molecule and the right electrode can be adjusted by opening and closing the junction.

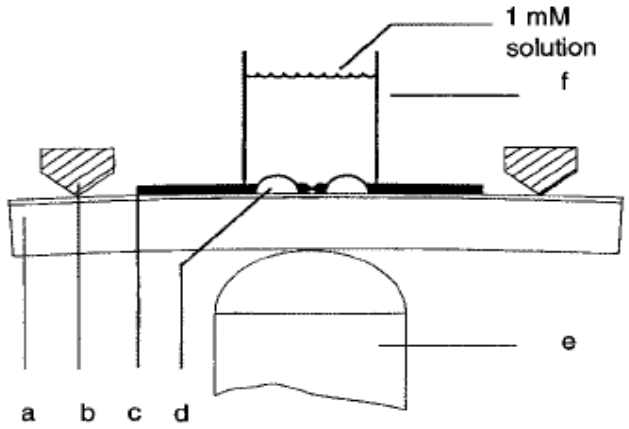

Fig. 1. A schematic of the MCB junction with (a) the bending beam, (b) the counter supports, (c) the notched gold wire, (d) the glue contacts, (e) the pizeo element, and (f) the glass tube containing the solution.

Four point technique

- Make quick measurements of conductivity on novel materials where contacts are not ideal

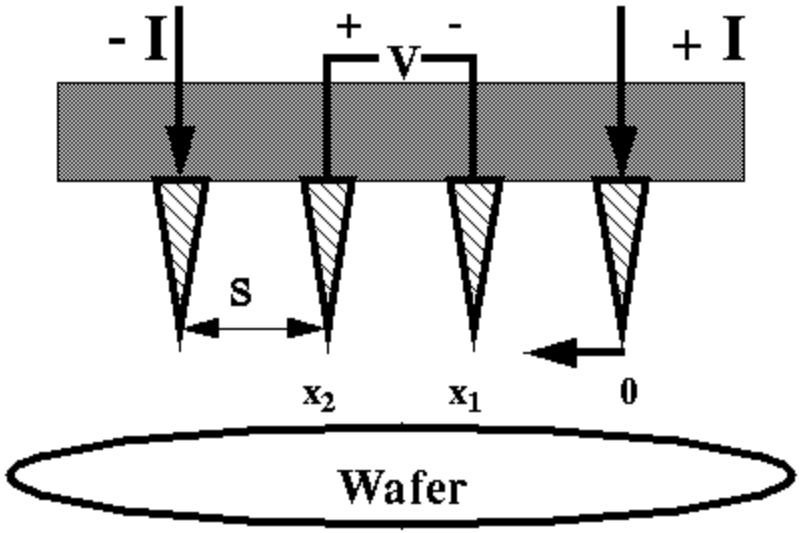

Bulk Sample $\rho = 2\pi s\left(\frac{V}{I}\right)$

$t >> s$

Thin Sheet $\rho = \frac{\pi t}{ln2}\left(\frac{V}{I}\right)$

thickness $t << s$

Typical probe spacing s ~ 1 mm

Capacitance Measurements

- Parallel plate capacitor

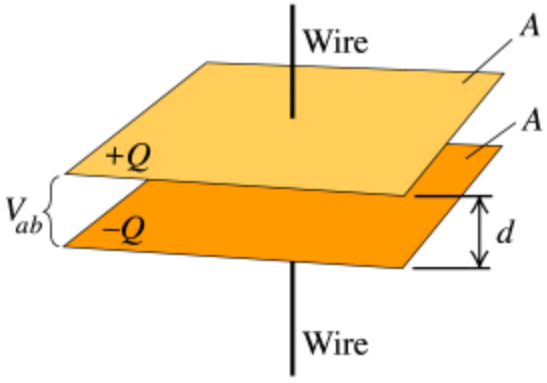

(a)

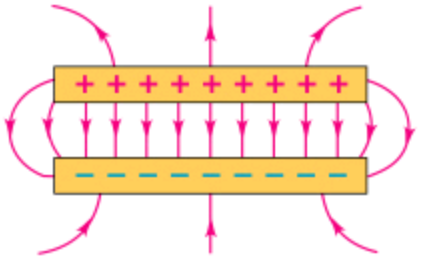

(b)

$$C = \frac{Q}{V}$$ Linear capacitor

$$C \approx \frac{\varepsilon A}{d}; A \gg d^2$$ Parallel plate

$$I = \frac{dQ}{dt} = C\frac{dV}{dt}$$

$$Z_C = \frac{V_C}{I_C} = \frac{-j}{2\pi f C} = -jX_C,$$

Dielectric constant can be measured if the dielectric thickness is known

Capacitance Spectroscopy

- When
  - semiconductors are used (surface potential and electric field are not linearly dependent)
  - the dielectric layer has electric field dependent conductivity (loss)
  - There are traps (or states) that can be charged and discharged only at certain voltages
- We can measure the small signal capacitance as a function of DC bias, and interpret C-V curves to gain information about the system

C-V characterization of MOS structures

- Measurement of C-V characteristics
  - Apply any dc bias, and superimpose a small (15 mV) ac signal
  - Generally measured at 1 MHz (high frequency) or at variable frequencies between 1KHz to 1 MHz
  - The dc bias V_G is slowly varied to get **quasi-continuous** C-V characteristics

Measured C-V characteristics on an n-type Si

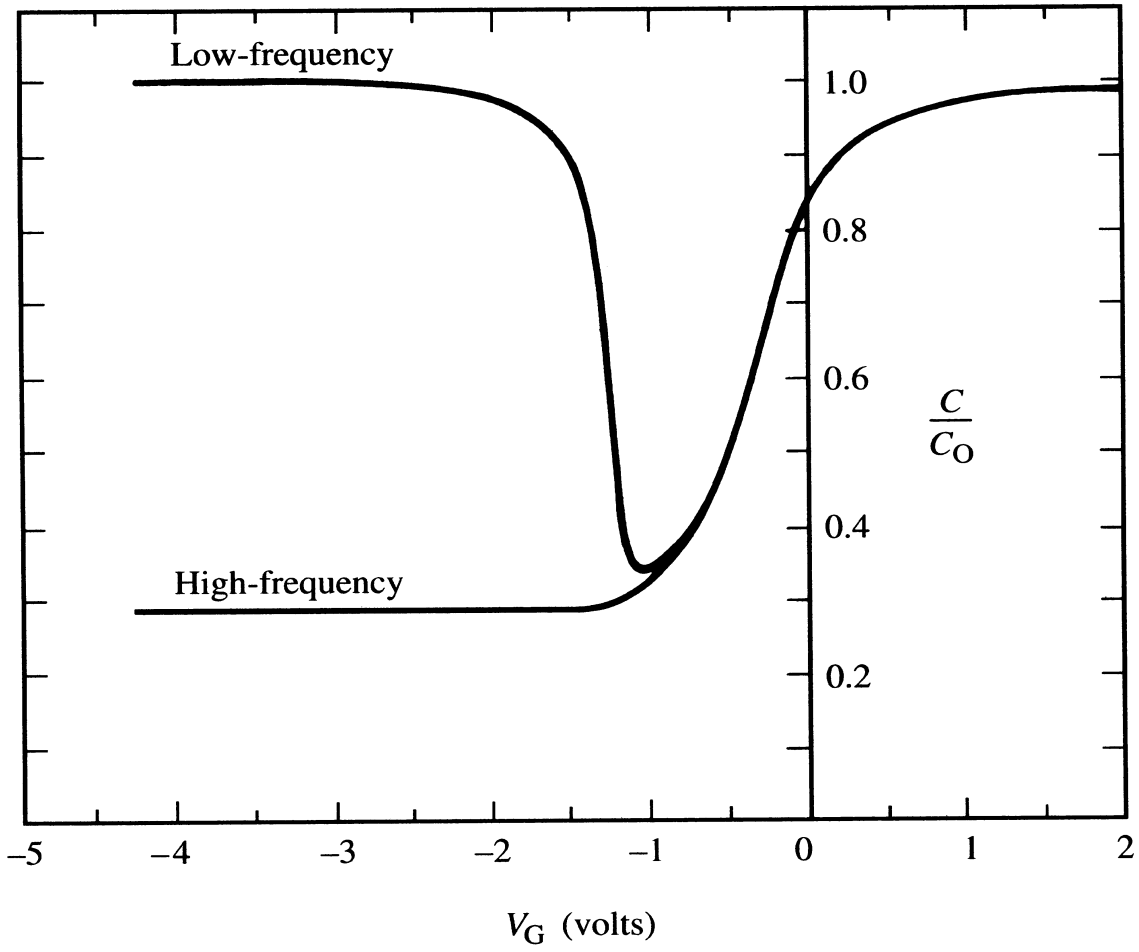

(b)

$N_D = 9.0 \times 10^{14}$ cm^{-3}

$x_{ox} = 0.119$ μm

Figure 16.11

Doping dependence of a MOS capacitor

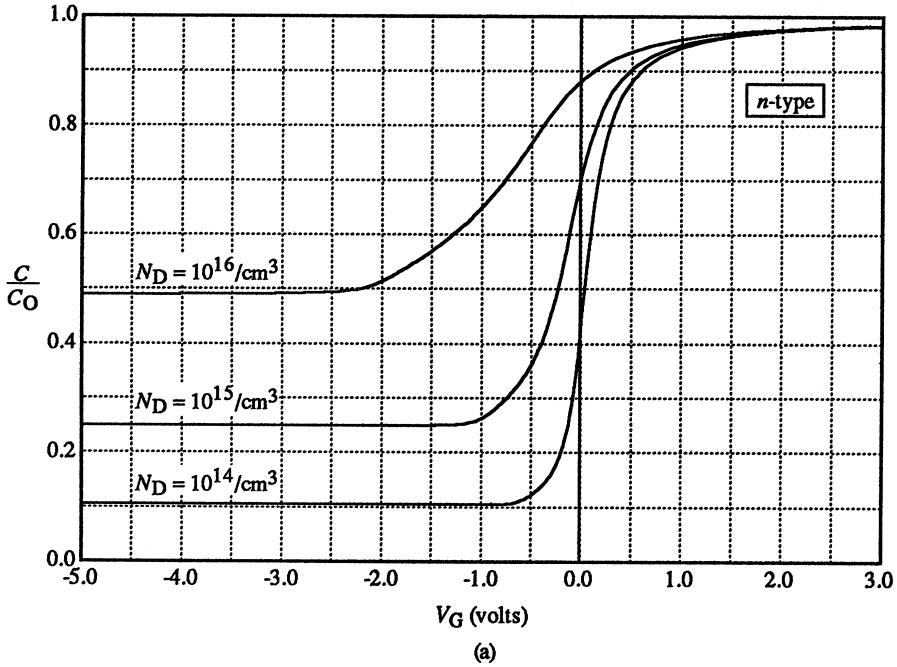

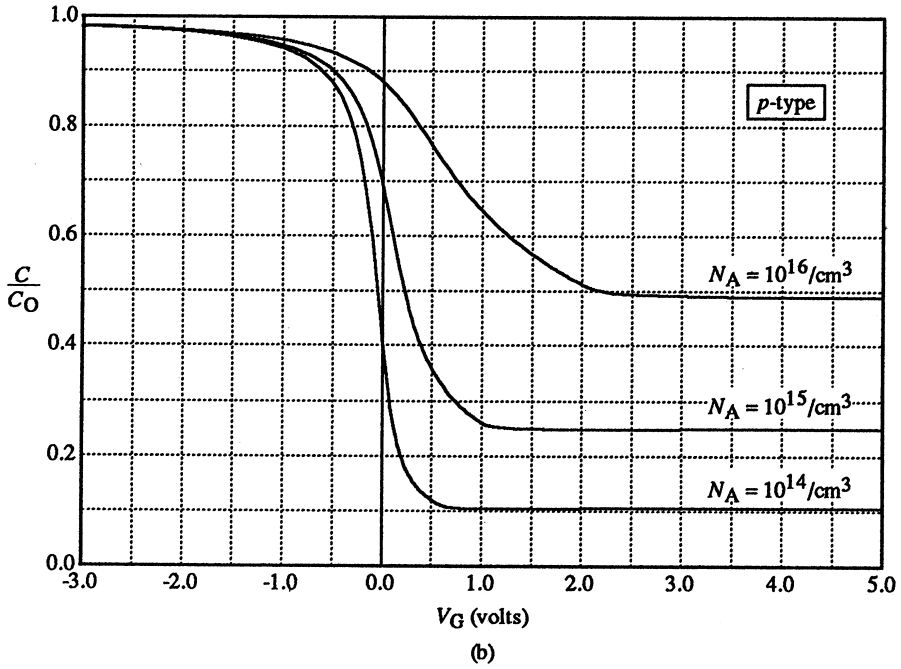

Figure 16.14

Can tell you carrier concentration, dielectric thickness or constant, Dielectric interface trap densities, Carrier diffusion properties etc.

2-D nanostructures:

graphene, metallic thin films, superlattices, … .

1-D nanostructures:

carbon nanotubes, quantum wires, conducting polymers, … .

0-D nanostructures:

semiconductor nanocrystals, metal nanoparticles,
lithographically patterned quantum dots, … .

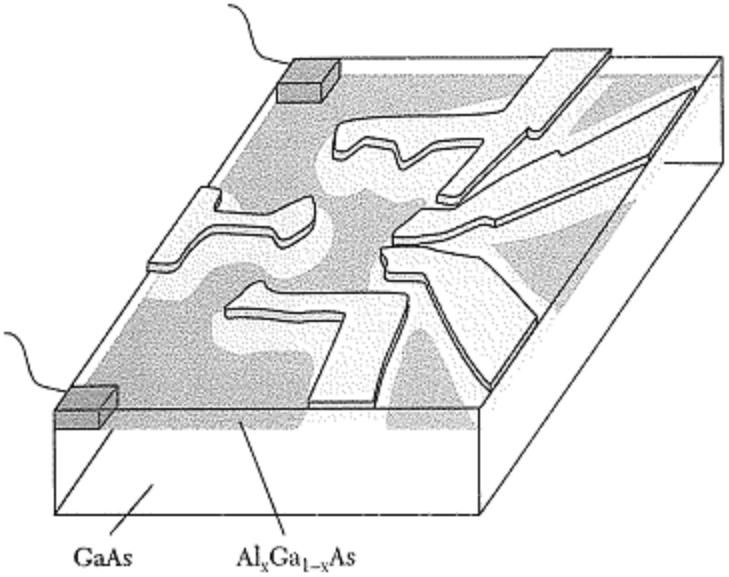

Gate electrode pattern
of a quantum dot

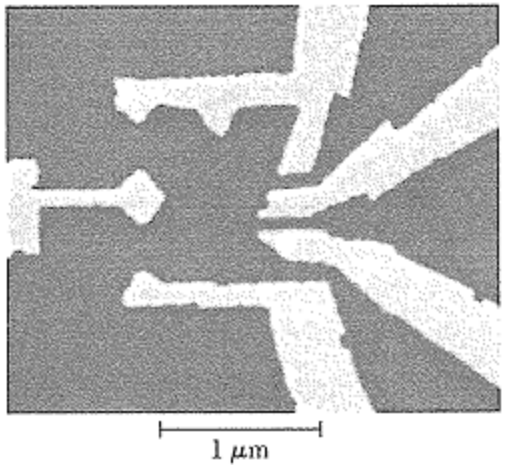

SEM image

2D electron gas (2DEG)

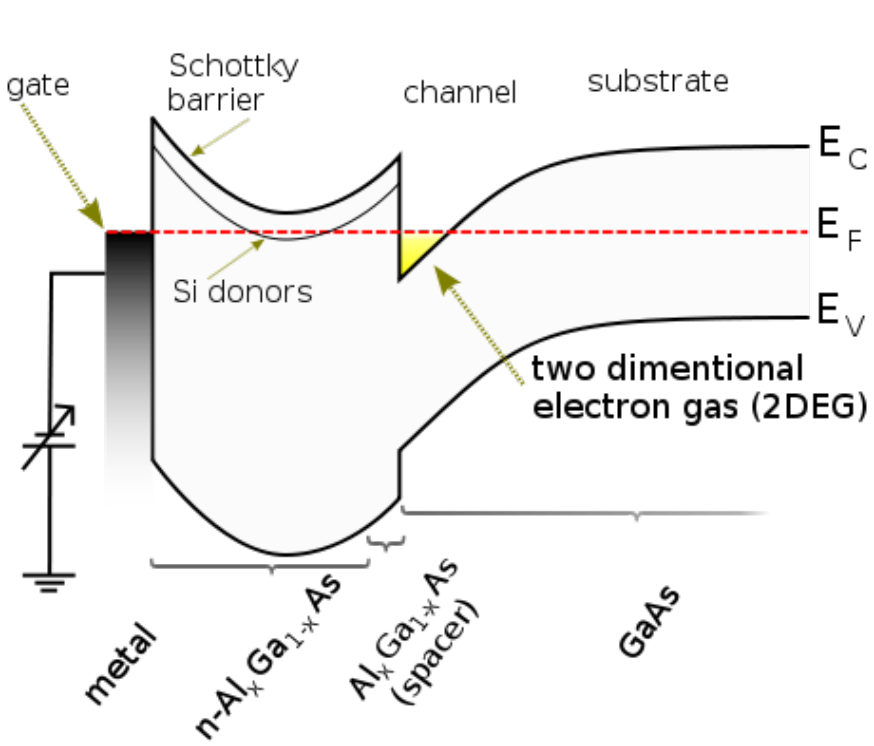

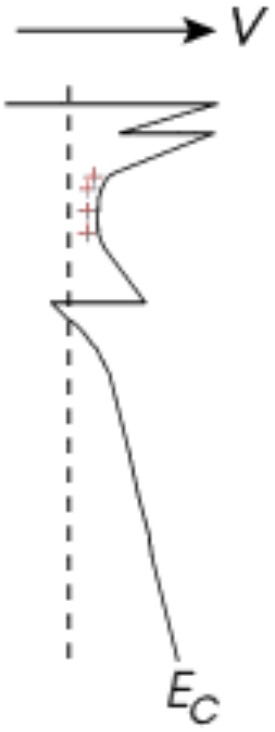

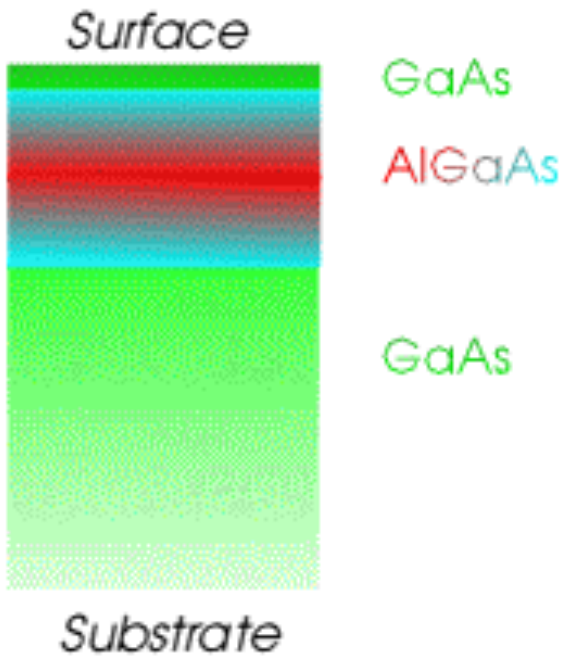

Historical landmarks of 2DEG mobility in GaAs.

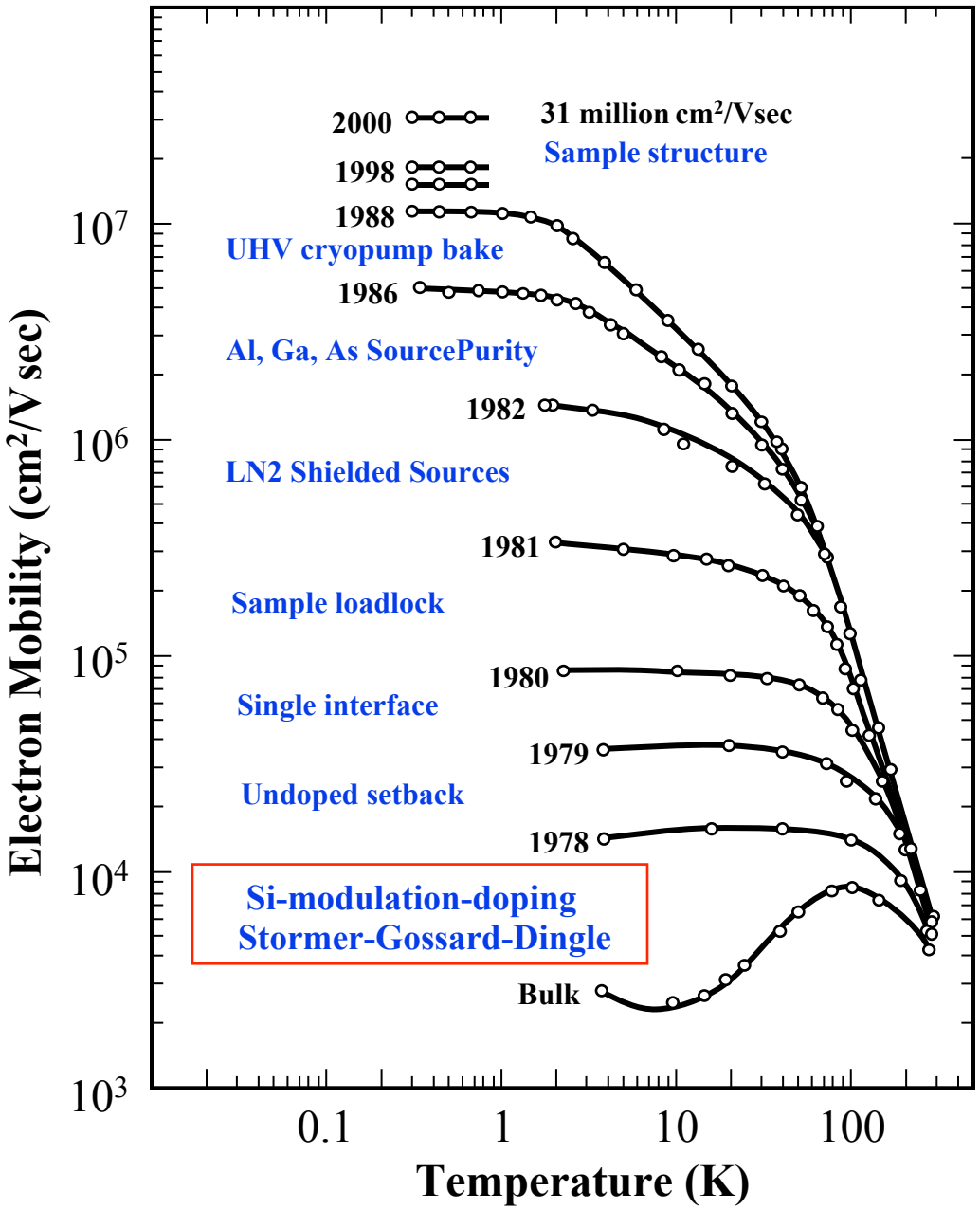

Electronic Structure of 2-D Systems

λ = de Broglie wavelength of electron
a = thickness of metal film

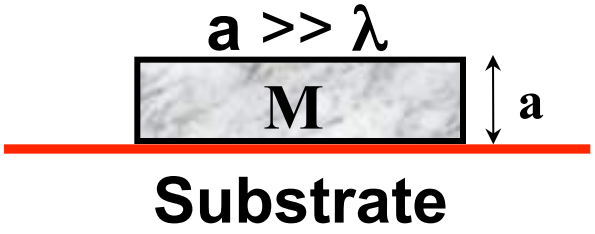

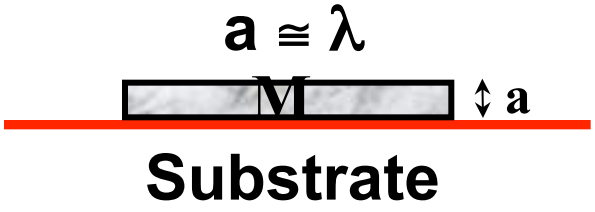

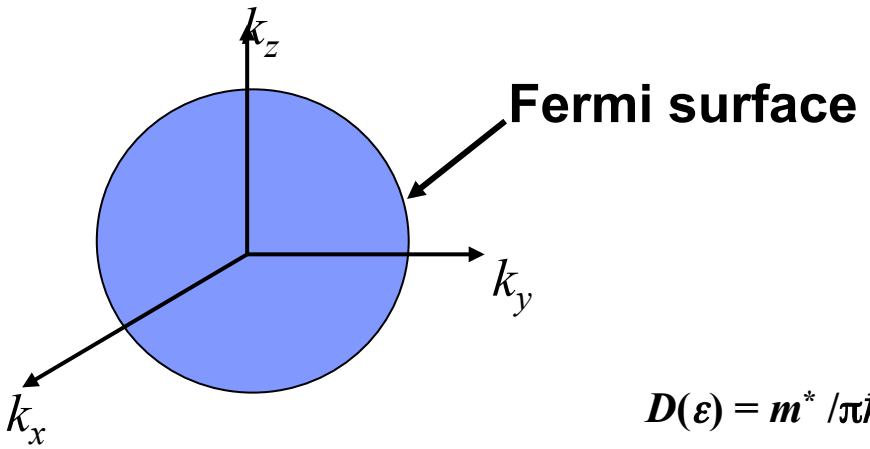

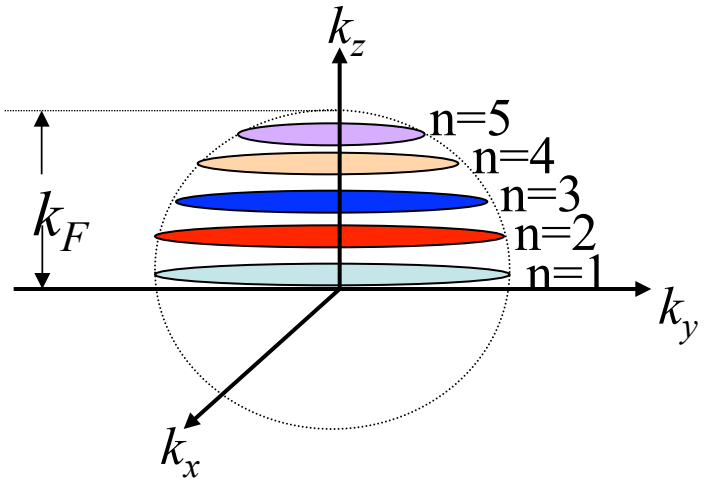

$D(\varepsilon) = m^* / \pi\hbar^2$

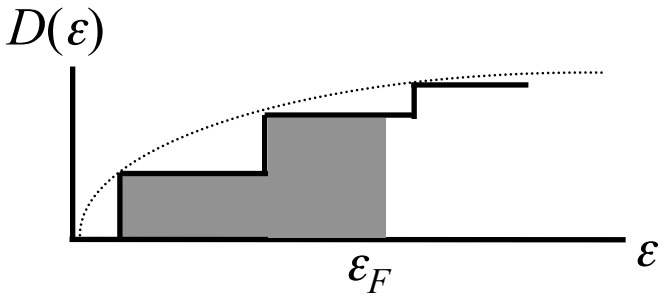

Classical Hall effect (1880 E.H. Hall)

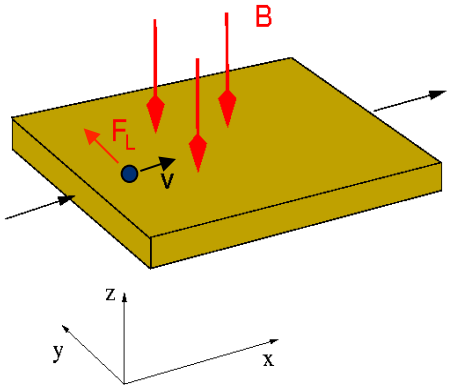

Lorentz-force on electron:

$$m\dot{\vec{v}} = -e\left(\vec{E} + \vec{v} \times \vec{B}\right) = 0 \qquad \Rightarrow \qquad \vec{E} = -\vec{v} \times \vec{B}$$

stationary current:

$$\vec{j} = -e\varrho\,\vec{v}$$

$$j_x = \frac{e\varrho}{B} E_y \qquad\qquad j_y = \frac{e\varrho}{B} E_x$$

Hall resistance:

$$R_{xy} \equiv \frac{E_y}{j_x} = \frac{1}{\nu}\frac{2\pi\hbar}{e^2}, \qquad\qquad R_{xx} = 0$$

$$\frac{1}{\nu} = \frac{e\,B}{2\pi\hbar\varrho} = \frac{B}{\Phi_D\varrho} \qquad\qquad \Phi_D = \frac{2\pi\hbar}{e}$$

Dirac flux quantum

2D electrons in magnetic fields: Landau levels

Hamiltonian: $$H = \frac{1}{2m}\left[(p_x + eA_x)^2 + (p_y + eA_y)^2\right]$$

coordinate transformation:

$$(x, p_x) \quad (y, p_y) \quad \longrightarrow \quad (X, Y) \quad (R_x, R_y)$$

center of cyclotron motion

radial vector of cyclotron motion

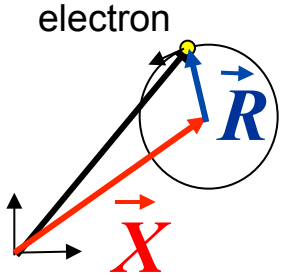

$$X = x - R_x \qquad Y = y - R_y$$

$$R_x = -\frac{p_y + eA_y}{eB} \qquad R_y = \frac{p_x + eA_x}{eB}$$

commutation relations:

$$[X, R_x] = [X, R_y] = [Y, R_x] = [Y, R_y] = 0$$

$$[X, Y] = -il_m^2 \qquad [R_x, R_y] = -il_m^2$$

$$l_m \equiv \sqrt{\frac{\hbar}{eB}}$$

2D electrons in magnetic fields: Landau levels

mapping to oscillator:

$$\hat{a} = \frac{1}{\sqrt{2}l_m}\left(R_y - iR_x\right) \qquad \hat{b} = \frac{1}{\sqrt{2}l_m}\left(X - iY\right)$$

$$[\hat{a}, \hat{a}^\dagger] = 1 \qquad [\hat{b}, \hat{b}^\dagger] = 1$$

$$H = \hbar\omega_c \; R^2 / 2\, l_m^{\,2} = \hbar\omega_c \; (\, a^+ a \; + ½ \,)$$

Landau levels

2D electrons in magnetic fields: Landau levels

typical scales:

- **length**

$$\langle R^2 \rangle_n = (1+2n) l_m^2$$

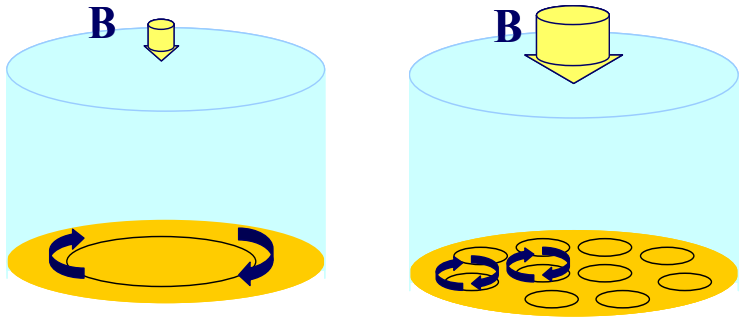

$$l_m \equiv \sqrt{\frac{\hbar}{eB}}$$

magnetic length

- **energy**

$$\hbar\omega_c = \frac{\hbar eB}{m} = \frac{l_m^2}{m}$$

cyclotron frequency

2D electrons in magnetic fields: Landau levels

degeneracy of Landau levels:

center of cyclotron motion (X, Y) arbitrary → degeneracy

- **2D density of states (DOS)**

$$\varrho_{\mathrm{DS}} = \frac{1}{2\pi l_m^2} = \frac{eB}{2\pi\hbar} = \frac{B}{\Phi_D}$$

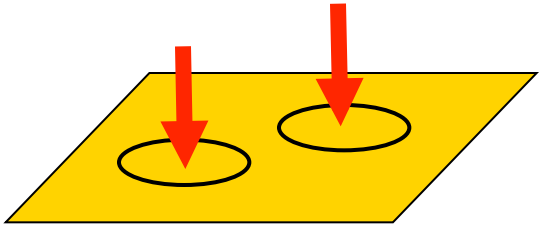

one state per area of cyclotron orbit

- **filling factor**

$$\nu = \frac{\varrho}{\varrho_{\mathrm{DS}}} = 2\pi l_m^2 \varrho = \frac{\rho \Phi_D}{B} = \frac{N}{N_\Phi}$$

atoms / # flux quanta

Quantum Hall effect

Quantization of conductivity
for a two-dimensional electron gas
at very low temperatures
in a high magnetic field.

$$\sigma = \nu \frac{e^2}{h}$$

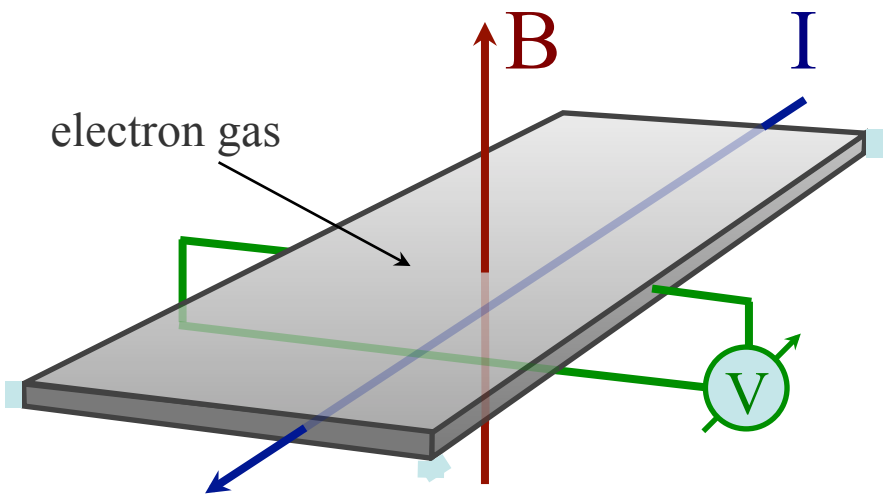

Semiconductor heterostructure confines
electron gas to two spatial dimensions.

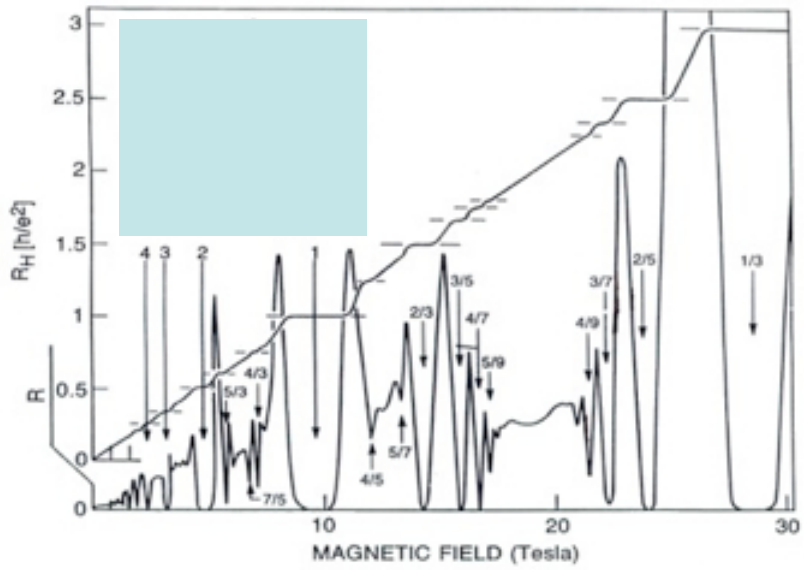

Quantum Hall states

Landau levels

$$E_n = h\frac{eB}{m}\left(n+\frac{1}{2}\right)$$

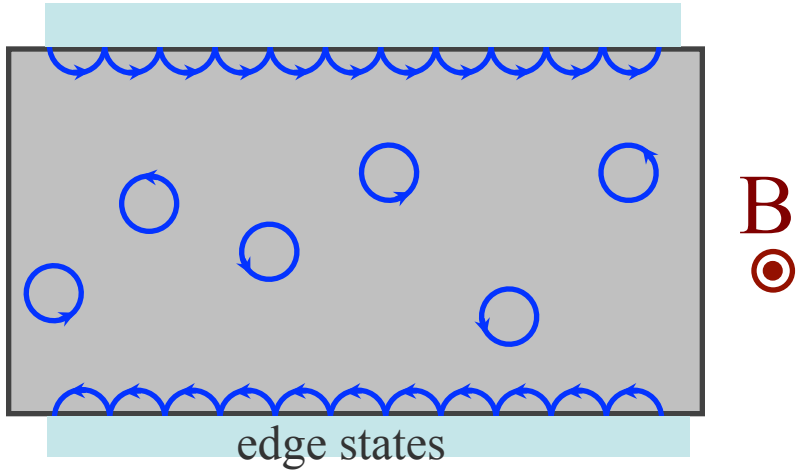

Landau level degeneracy

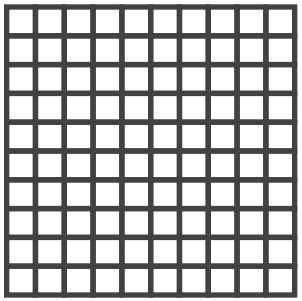

$2\Phi/\Phi_0$

orbital states

integer quantum Hall

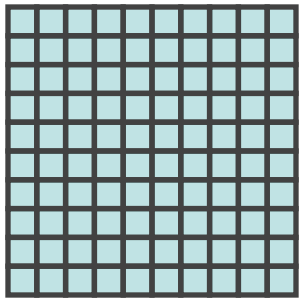

filled level

incompressible liquid

fractional quantum Hall

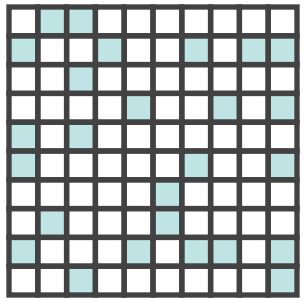

partially filled level

Coulomb repulsion

incompressible liquid

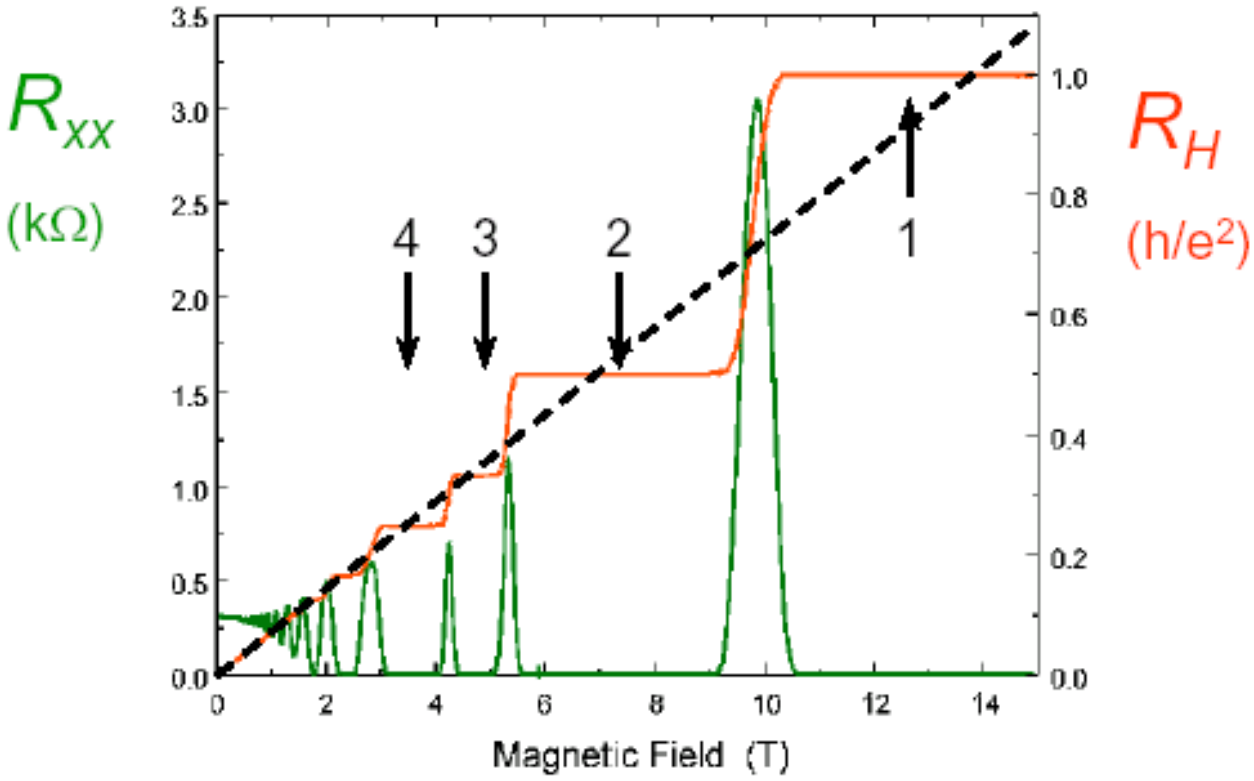
R_{xx}
(kΩ)
R_H
(h/e²)
4
3
2
1
Magnetic Field (T)
0.0
0.5
1.0
1.5
2.0
2.5
3.0
3.5
0.0
0.2
0.4
0.6
0.8
1.0
0
2
4
6
8
10
12
14

$$R_H = (1/\nu)(h/e^2)$$

Electronic Structure of 1-D Systems

$$\varepsilon = \varepsilon_{i,j} + \frac{\hbar^2 k^2}{2m} \qquad \psi(x,y,z) = \psi_{i,j}(x,y)e^{ikz}$$

i, j = quantum numbers in the cross section

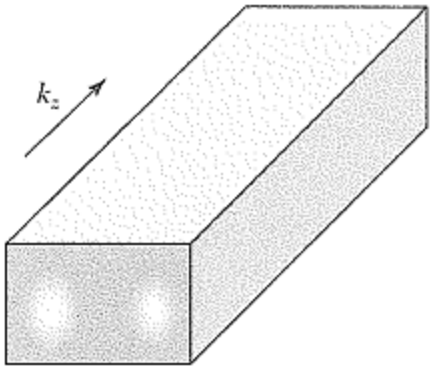

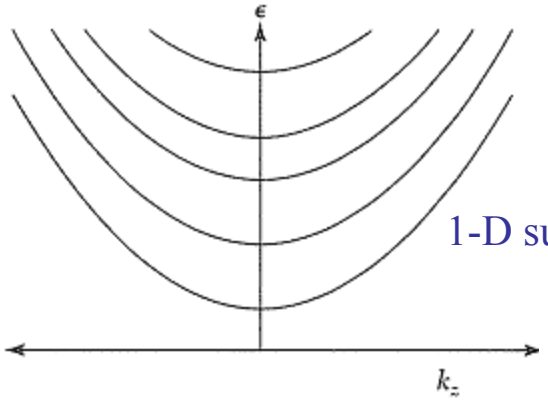

1-D subbands

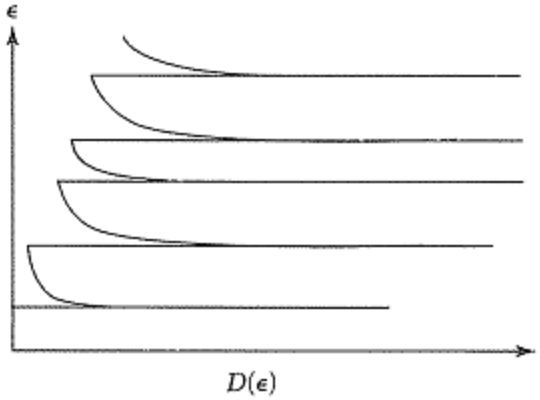

$$D(\varepsilon) = \sum_{i,j} D_{i,j}(\varepsilon) \qquad D_{i,j}(\varepsilon) = \frac{dN_{i,j}}{dk}\frac{dk}{d\varepsilon} = 2\times 2\frac{L}{2\pi}\sqrt{\frac{m}{2\hbar^2(\varepsilon-\varepsilon_{i,j})}} = \begin{cases} \dfrac{4L}{hv_{i,j}} & \varepsilon > \varepsilon_{i,j} \\ 0 & \varepsilon < \varepsilon_{i,j} \end{cases}$$

Let there be n_{1D} carriers per unit length, then $n_{1D} = \dfrac{2}{2\pi}2k_F = \dfrac{2}{\pi}k_F$

Fermi surface consists of 2 points at $k = \pm k_F$

Electrical Transport in 1-D

Conductance Quantization & the Landauer Formula

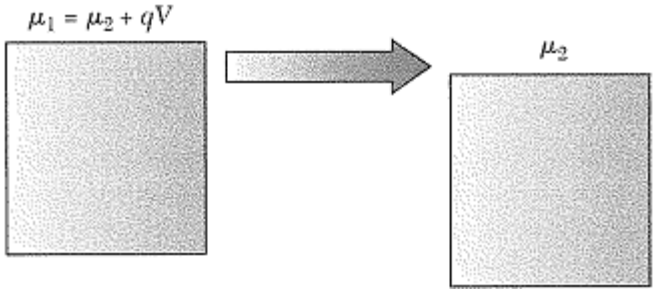

1-D channel with 1 occupied subband connecting 2 large reservoir.

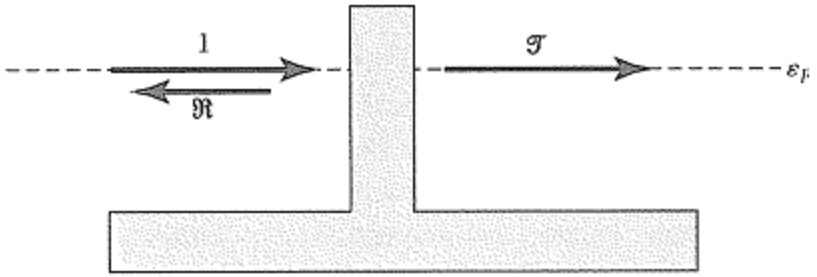

Barrier model for imperfect 1-D channel

Let Δn be the excess right-moving carrier density, $D_R(\varepsilon)$ be the corresponding DOS.

$$I = \Delta n\, qv = \frac{D_R(\varepsilon)\, q\, V}{L} qv = \frac{2}{hv} q^2 V v = \frac{2\, e^2}{h} V \qquad q = \pm e$$

→ The conductance quantum $G_Q = \dfrac{2\, e^2}{h}$ depends only on fundamental constants.

Likewise the resistance quantum $R_Q = \dfrac{1}{G_Q} = \dfrac{h}{2\, e^2}$

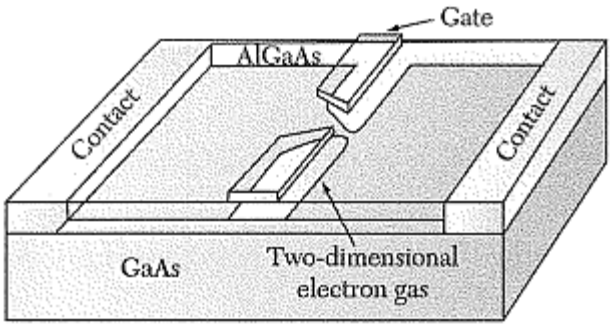

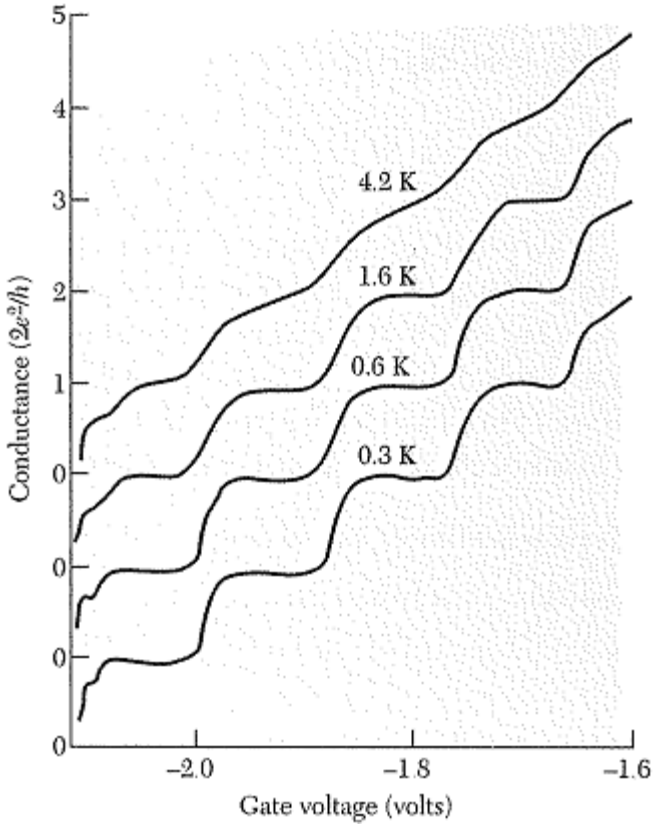

Channel fully depleted of carriers at $V_g = -2.1$ V.

If channel is not perfectly conducting,

$$G(\varepsilon_F) = \frac{2e^2}{h}\mathsf{T}(\varepsilon_F)$$ Landauer formula

T = transmission coefficient.

For multi-channel quasi-1-D systems

$$\mathsf{T}(\varepsilon_F) = \sum_{i,j} \mathsf{T}_{i,j}(\varepsilon_F)$$

i, j label transverse eigenstates.

For finite T,

$$I(\varepsilon_F, V, T) = \frac{2e^2}{h}\int_{-\infty}^{\infty} d\varepsilon \left[f_L(\varepsilon - eV) - f_R(\varepsilon)\right]\mathsf{T}(\varepsilon)$$

$$R = \frac{h}{2e^2\,\mathsf{T}} = \frac{h}{2e^2}\frac{\mathsf{T} + (1-\mathsf{T})}{\mathsf{T}} = \frac{h}{2e^2} + \frac{h}{2e^2}\frac{\mathsf{R}}{\mathsf{T}}$$

R = reflection coefficient.

Voltage Probes & the Buttiker-Landauer Formulism

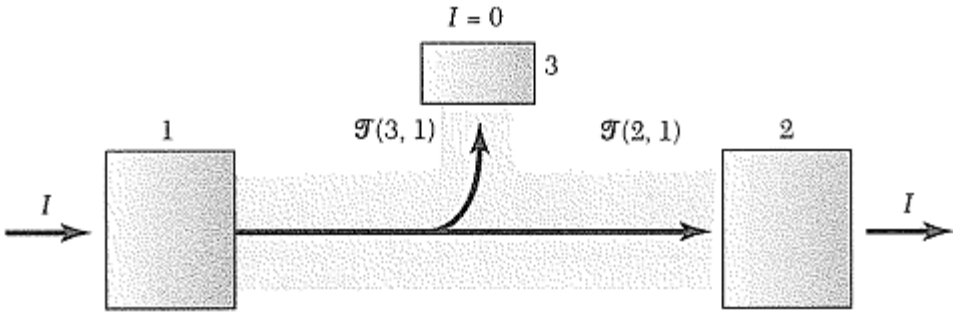

$\mathsf{T}^{(n,m)}$ = total transmission probability for an e to go from m to n contact.

1,2 are current probes; 3 is voltage probe.

For a current probe n with N channels, μ of contact is fixed by V.

Net current thru contact is $$I_n = \frac{2e^2}{h}\left(N_n V_n - \sum_m \mathsf{T}^{(n,m)} V_m \right)$$

Setting $I_n = 0$, $V_n = V \quad \forall n \quad \rightarrow \quad N_n = \sum_m \mathsf{T}^{(n,m)}$

For the voltage probe n, V_n adjusts itself so that $I_n = 0$.

$$\rightarrow \quad V_n = \frac{1}{N_n}\sum_m \mathsf{T}^{(n,m)} V_m = \frac{\sum_m \mathsf{T}^{(n,m)} V_m}{\sum_m \mathsf{T}^{(n,m)}}$$

$$\mu_n = \frac{\sum_m \mathsf{T}^{(n,m)} \mu_m}{\sum_m \mathsf{T}^{(n,m)}}$$

I_n , V_n depend on $\mathsf{T}^{(n,m)}$ $\rightarrow$ their values are path dependent.
Voltage probe can disturb existent paths.

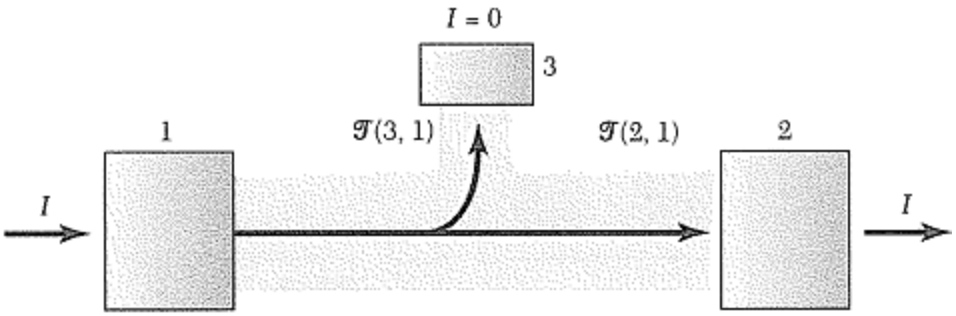

Let every *e* leaving 1 always arrive either at 2 or 3 with no back scattering.

$$V_3 = \frac{\mathsf{T}^{(3,1)} V}{\mathsf{T}^{(3,1)} + \mathsf{T}^{(3,2)}} = \frac{V}{2} \qquad \text{if} \quad \mathsf{T}^{(3,1)} = \mathsf{T}^{(3,2)}$$

Current out of 1: $$I = \frac{2e^2}{h}\left(V - \mathsf{T}^{(1,3)} V_3 \right) = \frac{2e^2}{h} V \left(1 - \frac{1}{2} \mathsf{T}^{(1,3)} \right) < \frac{2e^2}{h} V$$ no probe

Mesoscopic regime: $l_e < L < l_\varphi$.

Semi-classical picture: $t^{(m,n)} \propto \sum_j a_j \exp\left[\frac{i}{\hbar}\int_l^m \left(\mathbf{p} - \frac{e}{c}\mathbf{A}\right)\cdot d\mathbf{l}\right]$ $\qquad \mathsf{T}^{(n,m)} = \left| t^{(m,n)} \right|^2$

App. G

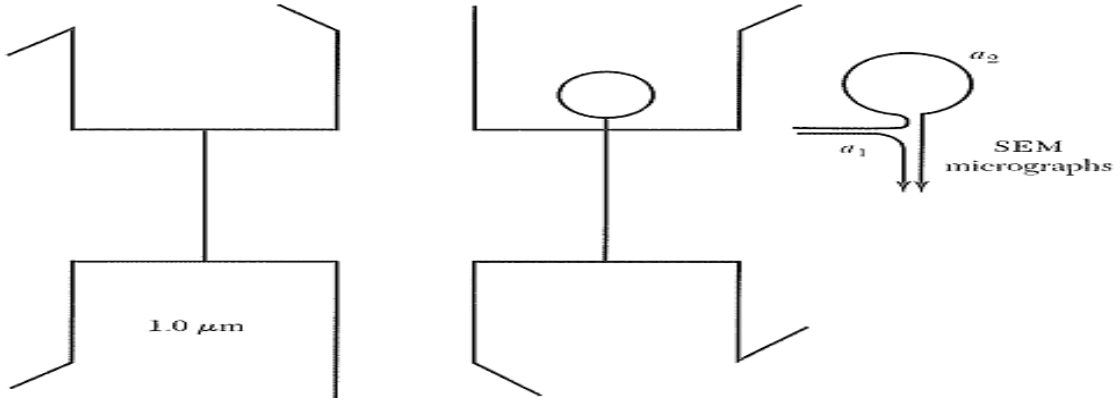

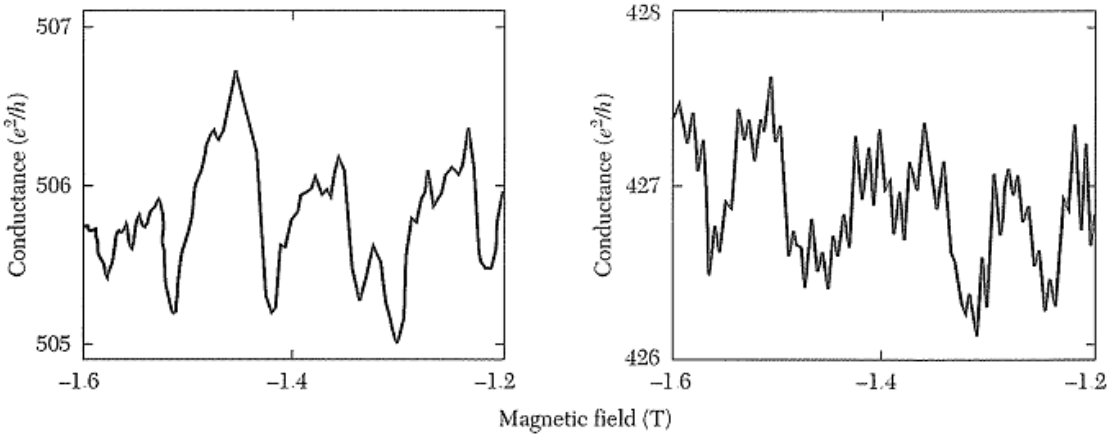

Aharonov-Bohm effect

$$\int_{loop} \mathbf{A}\cdot d\mathbf{l} = \int_S \nabla\times\mathbf{A}\cdot dS \quad = \Phi$$

$$\left| a_1 + a_2 \exp\left[\frac{ie}{\hbar c}\int_{loop} \mathbf{A}\cdot d\mathbf{l}\right]\right|^2 = \left| a_1 \right|^2 + \left| a_2 \right|^2 + 2\left| a_1 \right|\left| a_2 \right|\cos\left(\frac{2\pi\,\Phi}{hc/e}\right) \qquad \Phi_0 = \frac{hc}{e}$$

Localization

$$\mathsf{T} = \frac{|t_1|^2\,|t_2|^2}{1-2|r_1||r_2|\cos\varphi^* + |r_1|^2\,|r_2|^2} \quad \rightarrow \quad R = \frac{h}{2\,e^2\,\mathsf{T}} = \frac{h}{2e^2}\,\frac{1-2|r_1||r_2|\cos\varphi^* + |r_1|^2\,|r_2|^2}{|t_1|^2\,|t_2|^2}$$

$\langle \ldots \rangle$ = average over φ^* = average over k or ε .

$$\langle R\rangle = \frac{h}{2e^2}\,\frac{1+|r_1|^2\,|r_2|^2 - 2|r_1||r_2|\langle\cos\varphi^*\rangle}{|t_1|^2\,|t_2|^2} = \frac{h}{2e^2}\,\frac{1+|r_1|^2\,|r_2|^2}{|t_1|^2\,|t_2|^2}$$

larger than incoherent limit $\quad \frac{h}{2e^2}\,\frac{1-|r_1|^2\,|r_2|^2}{|t_1|^2\,|t_2|^2}$

Consider a long conductor consisting of a series of elastic scatterers of scattering length l_e .

Let $\langle R\rangle >> 1$, i.e., $\mathsf{R} \approx 1$ & $\mathsf{T} << 1$, ($\mathsf{R} + \mathsf{T} = 1$) .

For an additional length dL, $\quad d\mathsf{R} = \frac{dL}{l_e} \qquad d\mathsf{R} + d\mathsf{T} = 1$

Setting $\quad |r_1|^2 = \mathsf{R} \qquad |t_1|^2 = \mathsf{T} \qquad |r_2|^2 = d\mathsf{R} \qquad |t_2|^2 = d\mathsf{T}$

$$\rightarrow \quad \langle R + dR\rangle = \frac{h}{2e^2}\left(\frac{1+\mathsf{R}\;d\mathsf{R}}{\mathsf{T}\;d\mathsf{T}}\right) = \frac{h}{2e^2}\,\frac{1+\mathsf{R}\;d\mathsf{R}}{\mathsf{T}\,(1-d\mathsf{R})} = \frac{h}{2e^2\mathsf{T}}(1+\mathsf{R}\;d\mathsf{R})(1+d\mathsf{R}+\mathsf{L})$$

$$= \langle R\rangle\left[1+(\mathsf{R}+1)\,d\mathsf{R}+\mathsf{L}\right] \approx \langle R\rangle(1+2\,d\mathsf{R}+\mathsf{L}) = \langle R\rangle\left(1+2\,\frac{dL}{l_e}+\mathsf{L}\right)$$

$$\langle R + dR \rangle = \langle R \rangle \left(1 + 2 \frac{dL}{l_e} \right) \quad \rightarrow \quad \langle dR \rangle = \langle R \rangle \frac{2dL}{l_e}$$

$$\therefore \quad \ln \frac{\langle R \rangle}{\langle R \rangle_0} = \frac{2L}{l_e} \quad \text{where} \quad \langle R \rangle_0 = \langle R \rangle \big|_{L=0} = R_Q = \frac{h}{2e^2}$$

$$\langle R \rangle = \frac{h}{2e^2} \exp\left(\frac{2L}{l_e} \right) \qquad \text{C.f. Ohm's law } R \propto L$$

For a 1-D system with disorder, all states become localized to some length ξ.
Absence of extended states $\rightarrow$ $R \propto \exp(a L / \xi)$, a = some constant.
For quasi-1-D systems, one finds $\xi \sim N l_e$, where N = number of occupied subbands.

For $T > 0$, interactions with phonons or other e's reduce phase coherence to length $l_\varphi = A T^{-\alpha}$.

$$\therefore \quad \langle R \rangle \approx \frac{h}{2e^2} \exp\left(\frac{2l_\varphi}{l_e} \right) \qquad \text{for each coherent segment.}$$

Overall $\langle R \rangle \approx$ incoherent addition of L / l_φ such segments.

For sufficiently high T, $l_\varphi \leq l_e$, coherence is effectively destroyed & ohmic law is recovered.

All states in disordered 2-D systems are also localized.
Only some states (near band edges) in disordered 3-D systems are localized.

Conductance of a quantum point contact

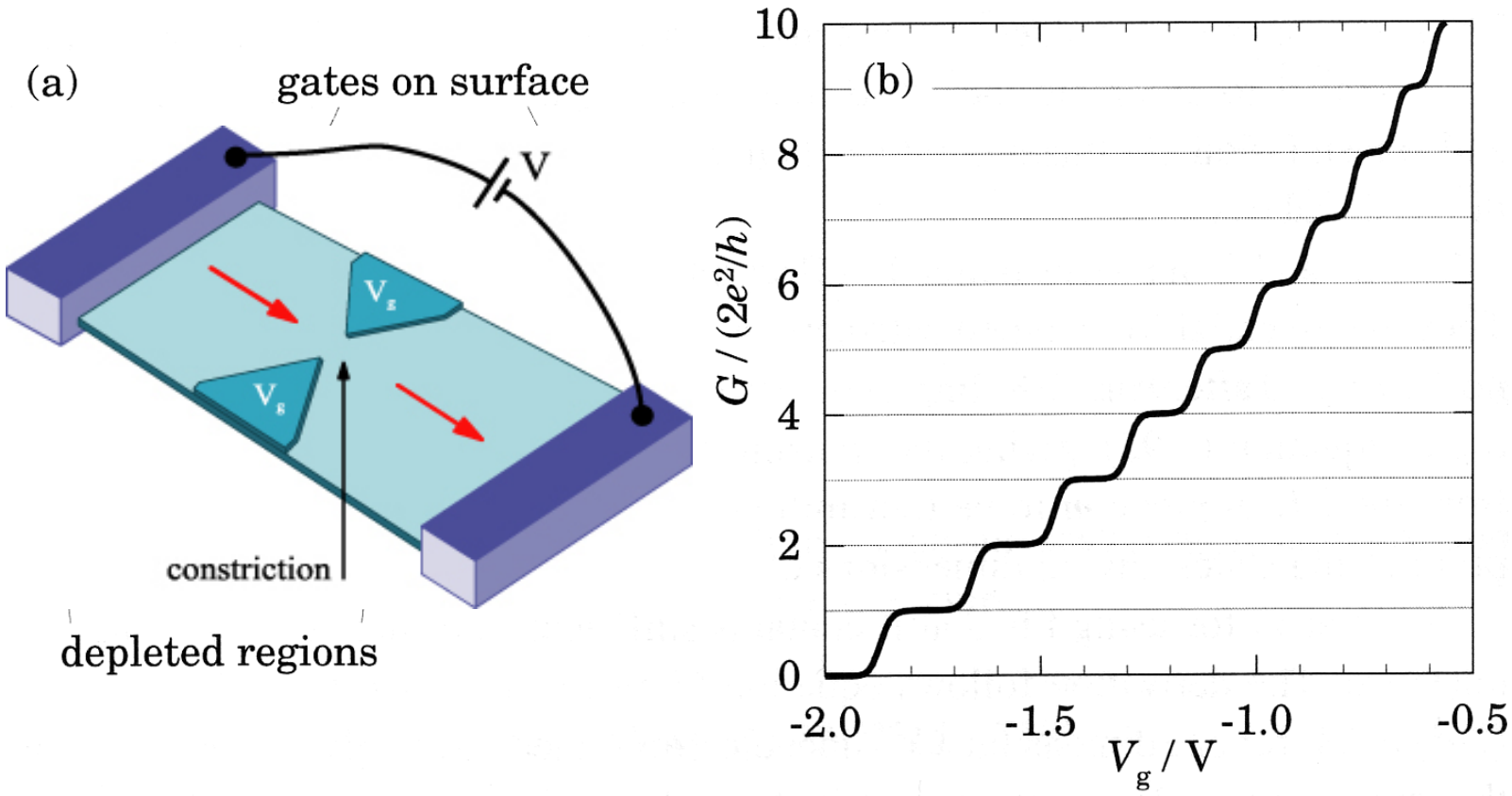

FIGURE 5.22. (a) Layout of a typical quantum point contact, a short constriction defined by patterned metal gates on the surface of a heterostructure containing a 2DEG. (b) Calculated conductance $G(V_g)$ as a function of gate voltage V_g. [From Nixon, Davies, and Baranger (1991).]

Quantum point contact

GaAs/AlGaAs interface :

two-dimensional electron gas

Quantum conductance

$$G = G_0 n$$

$$G_0 = \frac{2e^2}{h} = 7.75 \times 10^{-5}\,\Omega^{-1}$$

$$n = 1,2,3\cdots$$

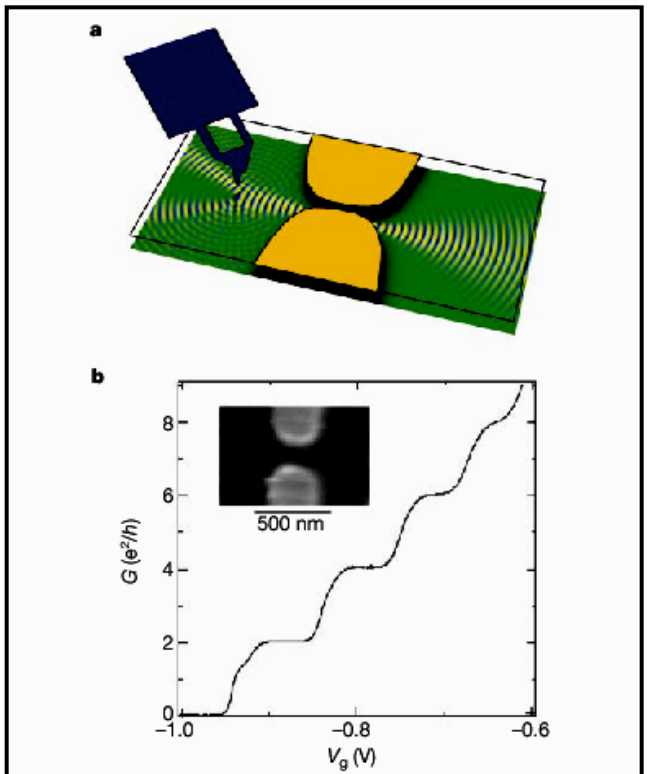

Figure 1 Experimental set-up. **a**, Schematic diagram of the experimental set-up used for imaging electron flow. The tip introduces a movable depletion region which scatters electron waves flowing from the quantum point contact (QPC). An image of electron flow is obtained by measuring the effect the tip has on QPC conductance as a function of tip position. Two ohmic contacts ~1 mm away from the QPC (not shown) allow the conductance of the QPC to be measured using an a.c. lock-in amplifier at 11 kHz. The root-mean-square voltage across the QPC, 0.2 mV, was chosen in order not to heat electrons significantly above the lattice temperature of 1.7 K. **b**, Conductance of the QPC used for Fig. 2b versus QPC width controlled by the gate voltage. Steps at integer multiples of $2e^2/h$ are clearly visible. The inset is a topographic AFM image of the QPC.

Electron flow close to a quantum point contact

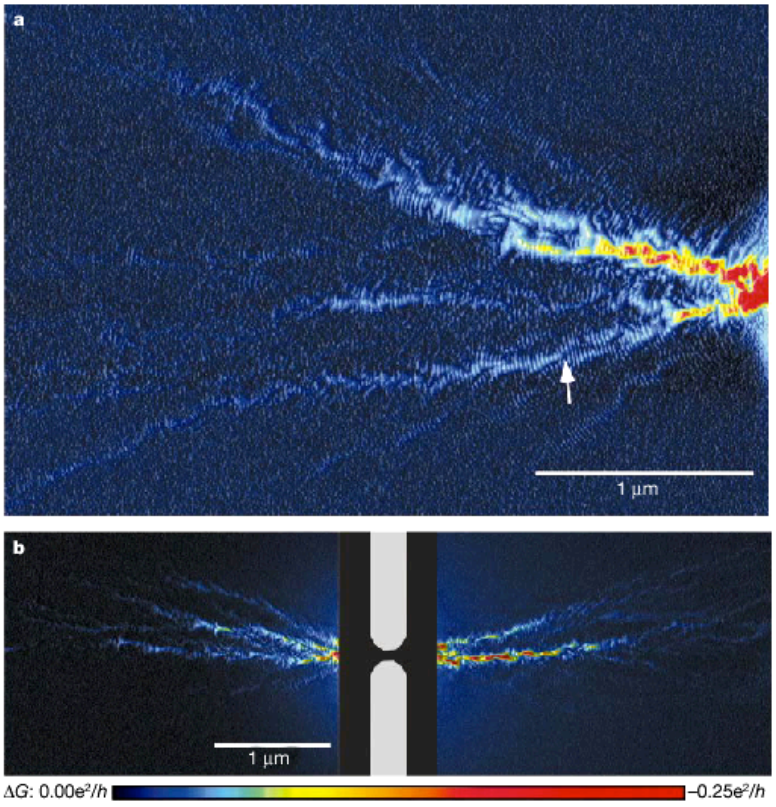

Figure 2 Experimental images of electron flow. **a**, Image of electron flow from one side of a QPC at $T = 1.7$ K, biased on the $G = 2e^2/h$ conductance step. Dark regions correspond to areas where the tip had little effect on QPC conductance, and hence are areas of low electron flow. The colour varies and the height in the scan increases with increasing electron flow. Narrow branching channels of electron flow are visible, and fringes spaced by $\lambda_F/2$, half the Fermi wavelength, are seen to persist across the entire scan. **b**, Images of electron flow from both sides of a different QPC, again biased on the $G = 2e^2/h$ conductance step. The gated region in the centre was not scanned. Strong channelling and branching are again clearly visible. The white arrow points out one example of the formation of a cusp downstream from a dip in the potential.

- Electrons are wave with wave vector k_F
- Interference stripe with

$$\lambda = \frac{1}{2k_F}$$

Quantum point contact formed in STM

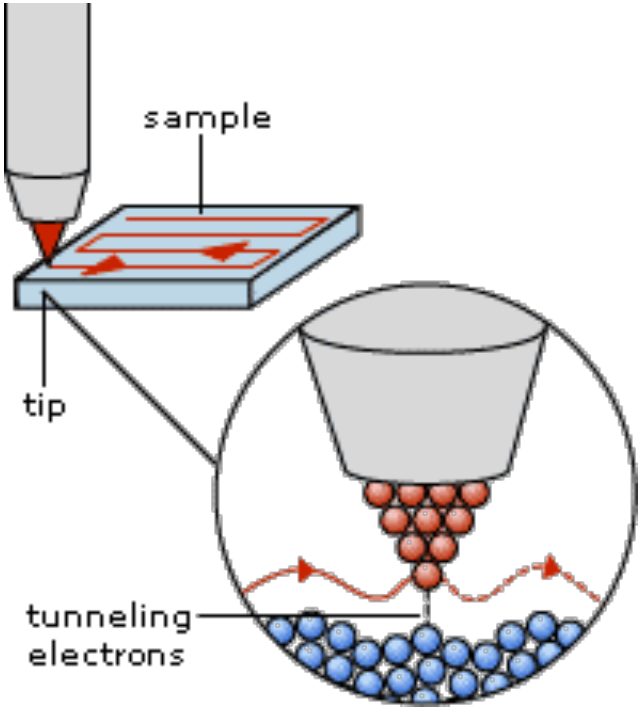

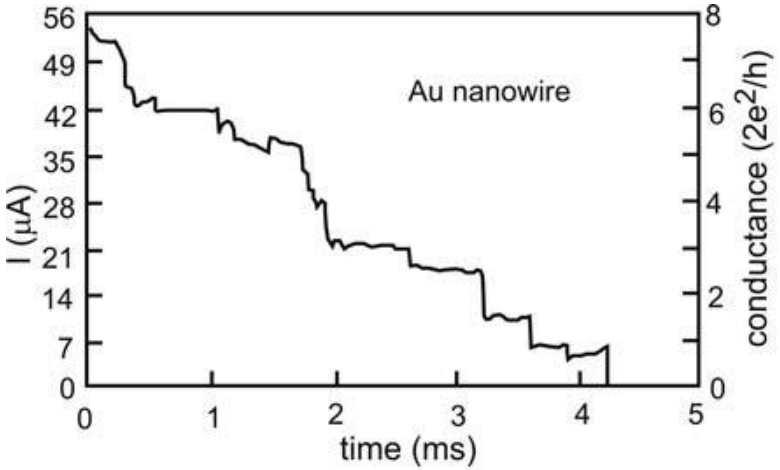

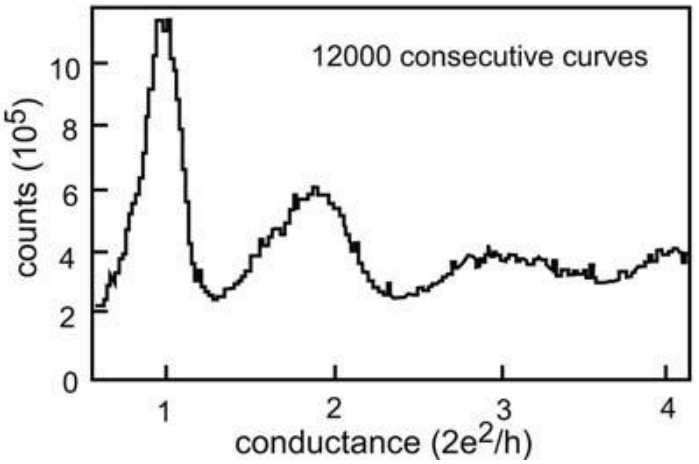

Electronic Structure of 0-D Systems

Quantum dots: Quantized energy levels.

e in spherical potential well: $\varepsilon_{n,l,m} = \varepsilon_{n,l}$ $\psi_{n,l,m}(r, \theta, \phi) = R_{n,l}(r)\, Y_{l,m}(\theta, \phi)$

For an infinite well with $V = 0$ for $r < R$:

$$\varepsilon_{n,l} = \frac{\mathrm{h}^2 \beta_{n,l}^2}{2m^* R^2} \qquad R_{n,l}(r) = j_l\left(\frac{\beta_{n,l}\, r}{R}\right) \qquad \text{for } r < R$$

$\beta_{n,\,l}$ = n^{th} root of $j_l(x)$. $j_l(\beta_{n,l}) = 0$

$\beta_{0,0} = \pi$ (1S), $\beta_{0,1} = 4.5$ (1P), $\beta_{0,2} = 5.8$ (1D)

$\beta_{1,0} = 2\pi$ (2S), $\beta_{1,1} = 7.7$ (2P)

Semiconductor Nanocrystals

CdSe nanocrystals

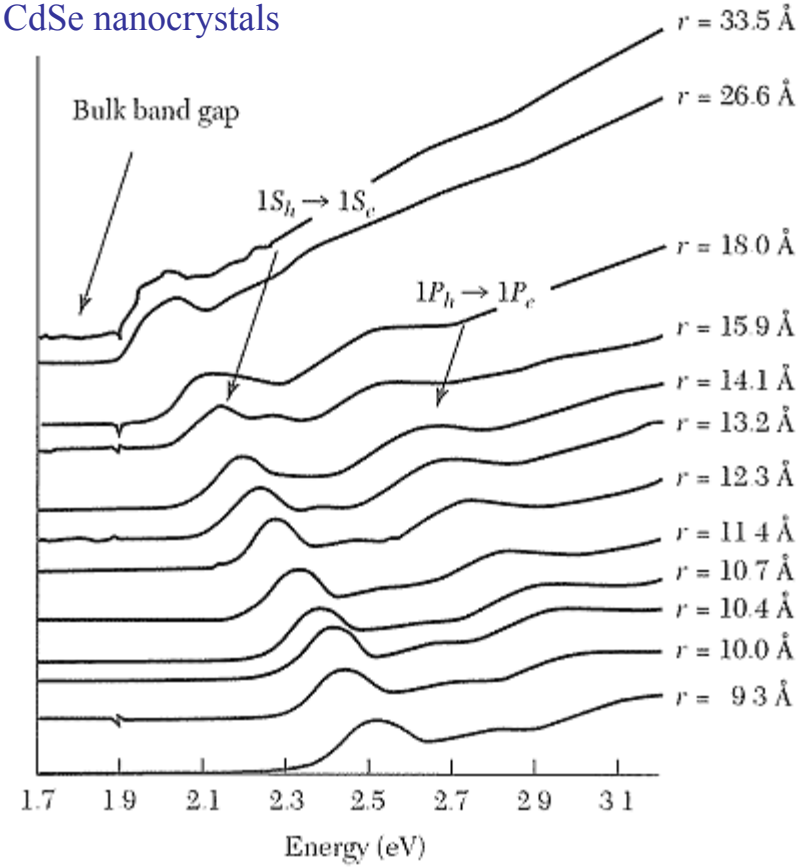

For CdSe:

$m_c^* = 0.13\, m$ $\qquad \varepsilon_{n,l} = \left(\frac{\beta_{n,l}}{\beta_{0,0}}\right)^2 \left(\frac{2.9eV}{R^2}\right)$

For $R = 2$ nm, $\qquad \varepsilon_{0,1} - \varepsilon_{0,0} = 0.76\, eV$

For e, $\varepsilon_{0,0}$ increases as R decreases.
For h, $\varepsilon_{0,0}$ decreases as R decreases.
$\rightarrow$ E_g increases as R decreases.

Optical spectra of nanocrystals can be tuned continuously in visible region.

Applications: fluorescent labeling, LED.

Kramers-Kronig relation: $\sigma''(\omega) = -\frac{2\omega}{\pi} P \int_0^\infty \frac{\sigma'(s)}{s^2 - \omega^2} ds$

For $\omega \rightarrow \infty$ $\qquad \sigma''(\omega) \approx \frac{ne^2}{m\omega} \approx \frac{2}{\pi\,\omega} \int_0^\infty \sigma'(s)\, ds \quad \rightarrow \quad \int_0^\infty \sigma'(s)\, ds = \frac{\pi\, n\, e^2}{2m}$ same as bulk

Strong transition at some ω in quantum dots $\rightarrow$ laser ?

Metallic Dots

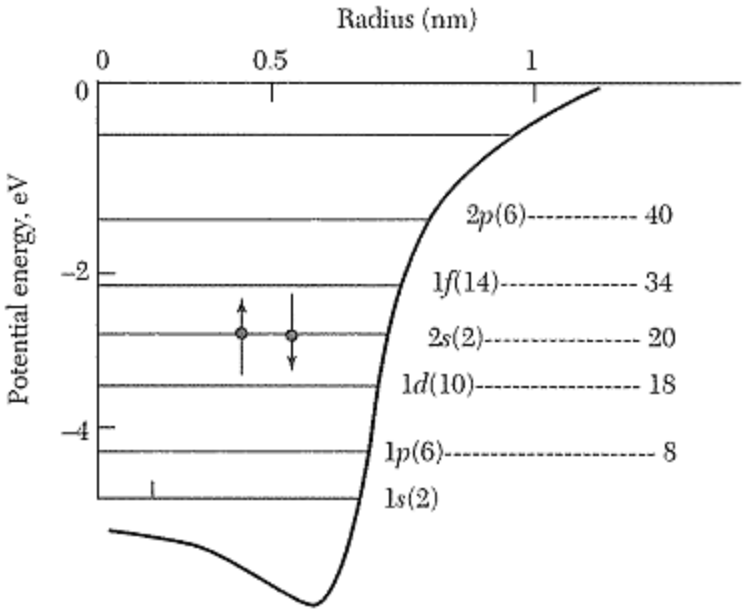

Small spherical alkali metallic cluster

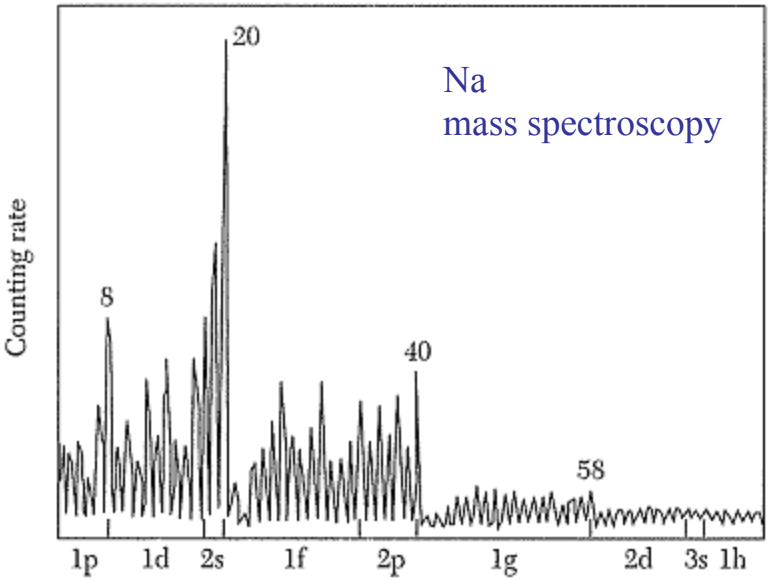

Mass spectroscopy (abundance spectra):
Large abundance at cluster size of magic numbers (8, 20, 40, 58, …)

→ enhanced stability for filled *e*-shells.

Average level spacing at ε_F :

$$\Delta\varepsilon \approx \frac{1}{D(\varepsilon_F)} = \frac{2\varepsilon_F}{3N}$$

For Au nanoparticles with $R = 2$ nm,
$\Delta\varepsilon \approx 2$ meV.
whereas CdSe gives $\Delta\varepsilon \approx 0.76$ eV.

→ ε quantization more influential in semiconductor.

Optical properties of metallic dots dominated by surface plasmon resonance.

If retardation effects are negligible, $$P = \frac{\chi}{1 + \frac{4\pi}{3}\chi} E_{ext}$$

$$\chi(\omega) = -\frac{n\,e^2}{m\,\omega^2} \quad \rightarrow \quad P = \frac{1}{\frac{m\,\omega^2}{n\,e^2} - \frac{4\pi}{3}} E_{ext} = \frac{3}{4\pi\left(\frac{3\,\omega^2}{\omega_p^2} - 1\right)} E_{ext}$$

Surface plasma mode at singularity: $\omega_{sp} = \frac{\omega_p}{\sqrt{3}}$ indep of R.

For Au or Ag, $\omega_p \sim$ UV, $\omega_{sp} \sim$ Visible.

→ liquid / glass containing metallic nanoparticles are brilliantly colored.

Large **E** just outside nanoparticles near resonance enhances weak optical processes. This is made use of in Surface Enhanced Raman Scattering (SERS), & Second Harmonic Generation (SHG).

Discrete Charge States

Thomas-Fermi approximation: $\mu_{N+1} = \varepsilon_{N+1} - e\varphi \quad = \varepsilon_{N+1} + NU - \alpha e V_g$

U = interaction between 2 e's on the dot = charging energy.
α = rate at which a nearby gate voltage V_g shifts φ of the dot.

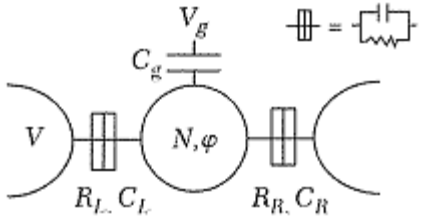

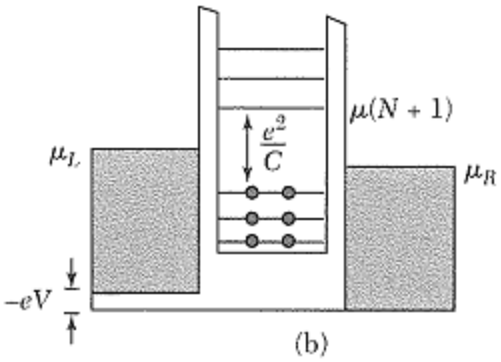

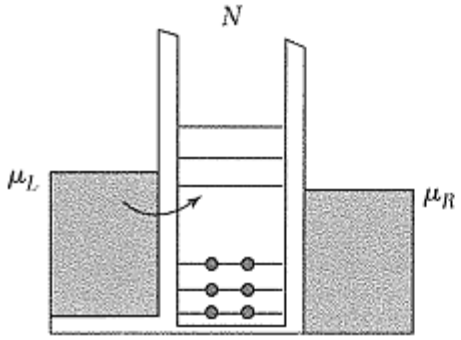

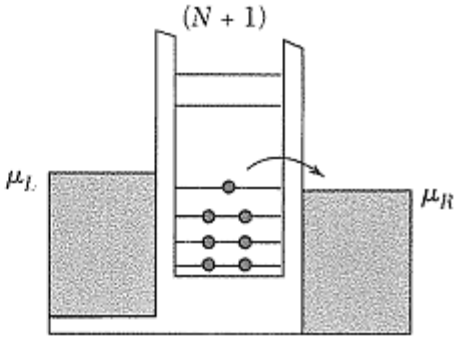

Neglecting its dependence on state,

$$U = \frac{e^2}{C} \qquad \alpha = \frac{C_g}{C}$$

C = capacitance of dot.
C_g = capacitance between gate & dot

If dot is in weak contact with reservoir, e's will tunnel into it until the μ's are equalized.

Change in V_g required to add an e is

$$\Delta V_g = \frac{1}{\alpha e}\left(\varepsilon_{N+1} - \varepsilon_N + \frac{e^2}{C} \right)$$

U depends on size &shape of dot & its local environment.

For a spherical dot of radius R surrounded by a spherical metal shell of radius $R + d$,

$$U = \frac{e^2}{\varepsilon} \frac{d}{R} \frac{}{R+d}$$

For $R = 2$ nm, $d = 1$ nm & $\varepsilon = 1$, we have

$U = 0.24$ eV $>>$ $k_B T = 0.026$eV at $T = 300$K

$\rightarrow$ Thermal fluctuation strongly supressed.

For metallic dots of 2nm radius, $\Delta\varepsilon \approx 2$meV $\rightarrow$ ΔV_g due mostly to U.
For semiC dots, e.g., CdSe, $\Delta\varepsilon \approx 0.76$ eV $\rightarrow$ ΔV_g due both to $\Delta\varepsilon$ & U.

Charging effect is destroyed if tunneling rate is too great.
Charge resides in dot for time $\delta t \approx RC$. (R = resistance)

$\rightarrow$ $$\delta\varepsilon \approx \frac{h}{\delta t} \approx \frac{h}{RC} = \frac{e^2}{C} \frac{h}{e^2} \frac{1}{R}$$

Quantum fluctuation smears out charging effect when $\delta\varepsilon \approx U$, i.e., when $R \sim h / e^2$.

Conditions for a Coulomb Blockade

1) The Coulomb energy e^2/C needs to exceed the thermal energy k_BT.

Otherwise an extra electron can get onto the dot with thermal energy instead of being blocked by the Coulomb energy. A dot needs to be either small (<10 nm at 300K) or cold (< 1K for a μm sized dot).

2) The residence time $\Delta t = RC$ of an electron on the dot needs to be so long that the corresponding energy uncertainty $\Delta E = h/\Delta t = h/RC$ is less than the Coulomb energy e^2/C. That leads to a condition for the tunnel resistance between the dot and source /drain: $R > h/e^2 \approx 26\ k\Omega$

Electrical Transport in 0-D

For $T < (U + \Delta\varepsilon) / k_B$, U & $\Delta\varepsilon$ control e flow thru dot.

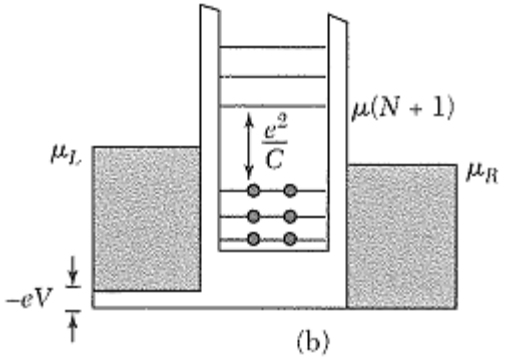

Transport thru dot is suppressed when μ_L & μ_R of leads lie between μ_N & μ_{N+1} (Coulomb blockade)

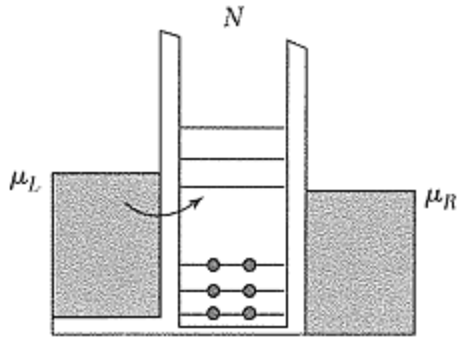

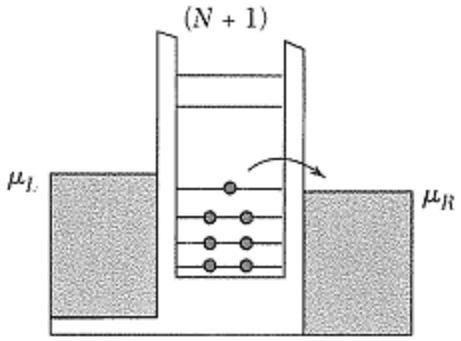

Transport is possible only when μ_{N+1} lies between μ_L & μ_R .

→ Coulomb oscillations of $G(V_g)$.

Coulomb Oscillations

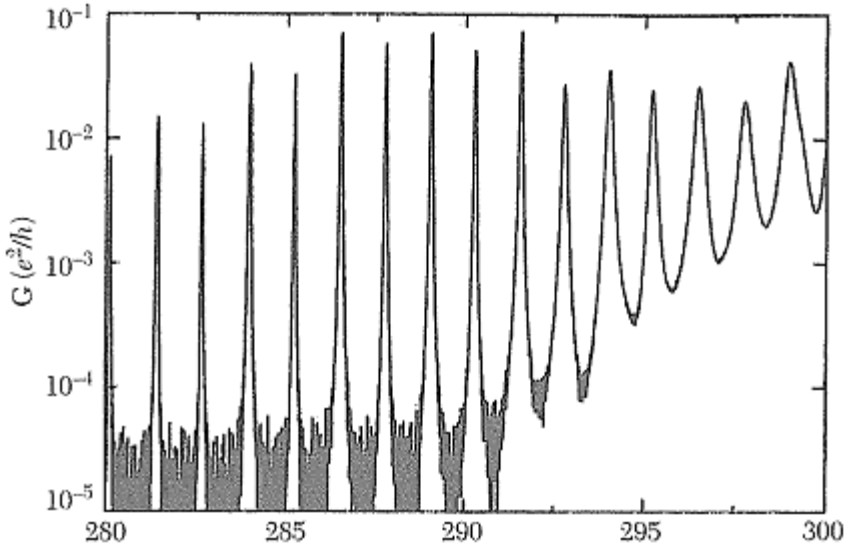

GaAs/AlGaAs
$T = 0.1$K

$$\Delta V_g = \frac{1}{\alpha e}\left(\varepsilon_{N+1} - \varepsilon_N + \frac{e^2}{C} \right)$$

Coulomb oscillation occurs whenever $U > k_B T$, irregardless of $\Delta\varepsilon$.

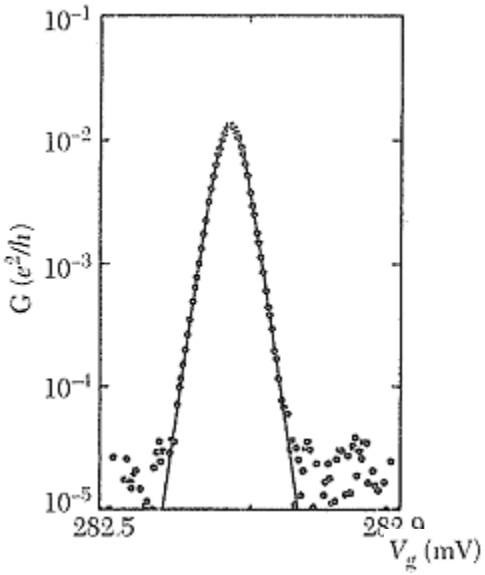

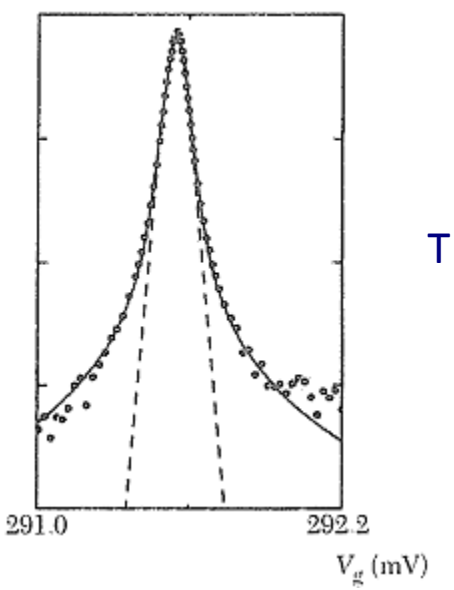

For $\Delta\varepsilon >> k_B T$, c.f. resonant tunneling:

$$\mathsf{T} = \frac{|t_1|^2 |t_2|^2}{1 - 2|r_1||r_2|\cos(2kL + \varphi_{r1} + \varphi_{r2}) + |r_1|^2 |r_2|^2}$$

$$\mathsf{T}(\varepsilon) = \frac{4\Gamma_1 \Gamma_2}{(\Gamma_1 + \Gamma_2)^2 + 4(\varepsilon - \varepsilon_n)^2}$$

Thermal broadening

Breit-Wigner lineshape

Single Electron Transistor (SET)

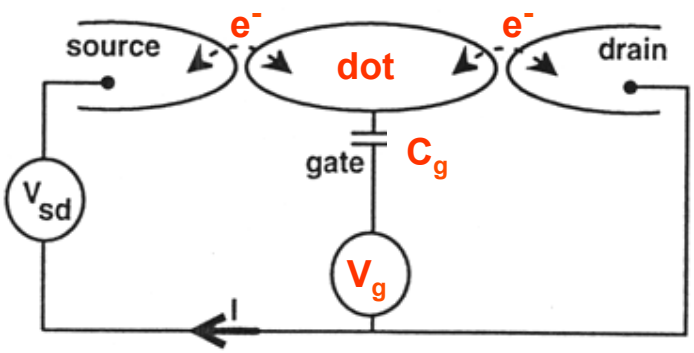

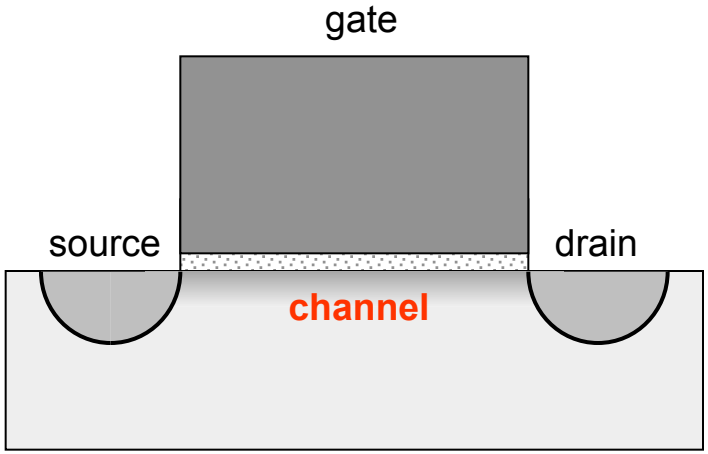

A single electron transistor is similar to a normal transistor (below), except

1) **the channel is replaced by a small dot.**

2) **the dot is separated from source and drain by thin insulators.**

An electron tunnels in two steps:

source → dot → drain

The gate voltage V_g is used to control the charge on the gate-dot capacitor C_g .

How can the charge be controlled with the precision of a single electron?

Kouwenhoven et al., *Few Electron Quantum Dots*, Rep. Prog. Phys. **64**, 701 (2001).

Designs for Single Electron Transistors

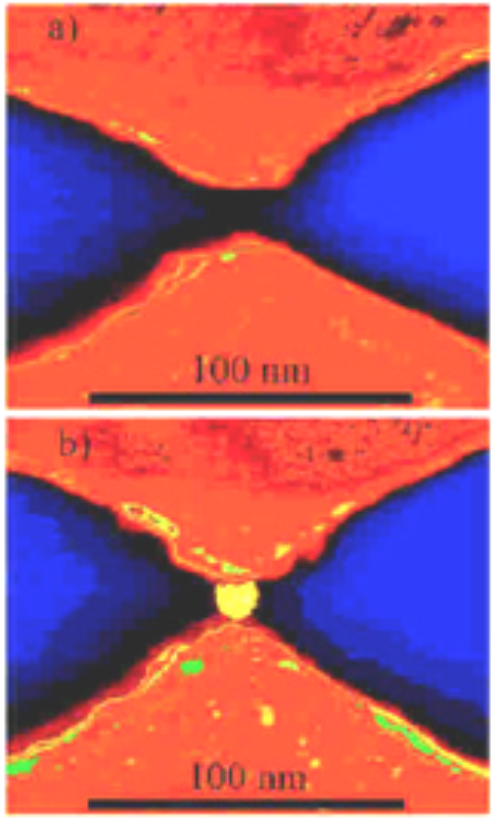

Nanoparticle attracted electrostatically to the gap between source and drain electrodes. The gate is underneath.

1 Vertical quantum dot structure

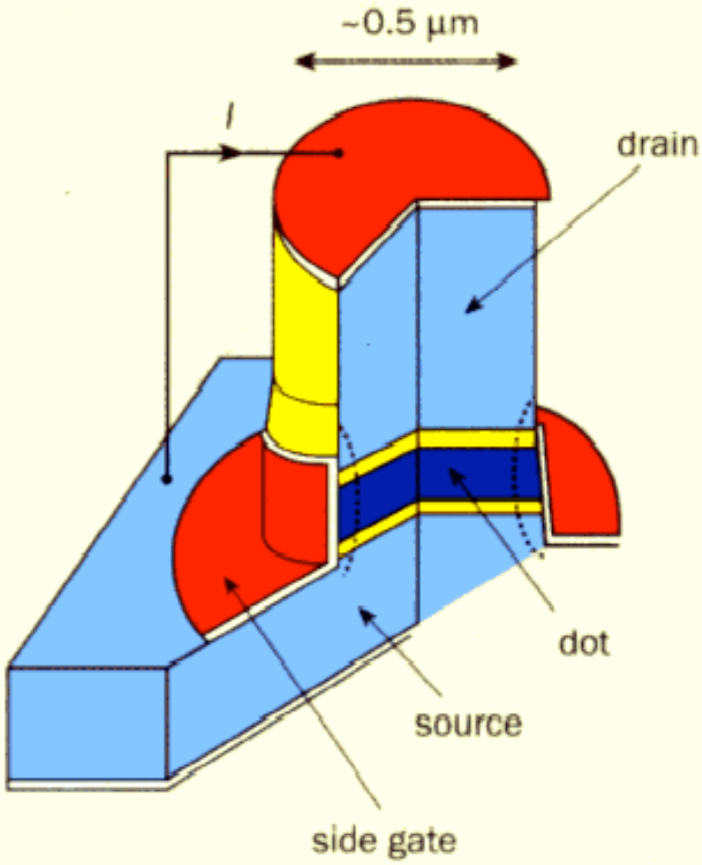

The quantum-dot structure studied at Delft and NTT in Japan is fabricated in the shape of a round pillar. The source and drain are doped semiconductor layers that conduct electricity, and are separated from the quantum dot by tunnel barriers 10 nm thick. When a negative voltage is applied to the metal side gate around the pillar, it reduces the diameter of the dot from about 500 nm to zero, causing electrons to leave the dot one at a time.

Two Step Tunneling

source → dot → drain

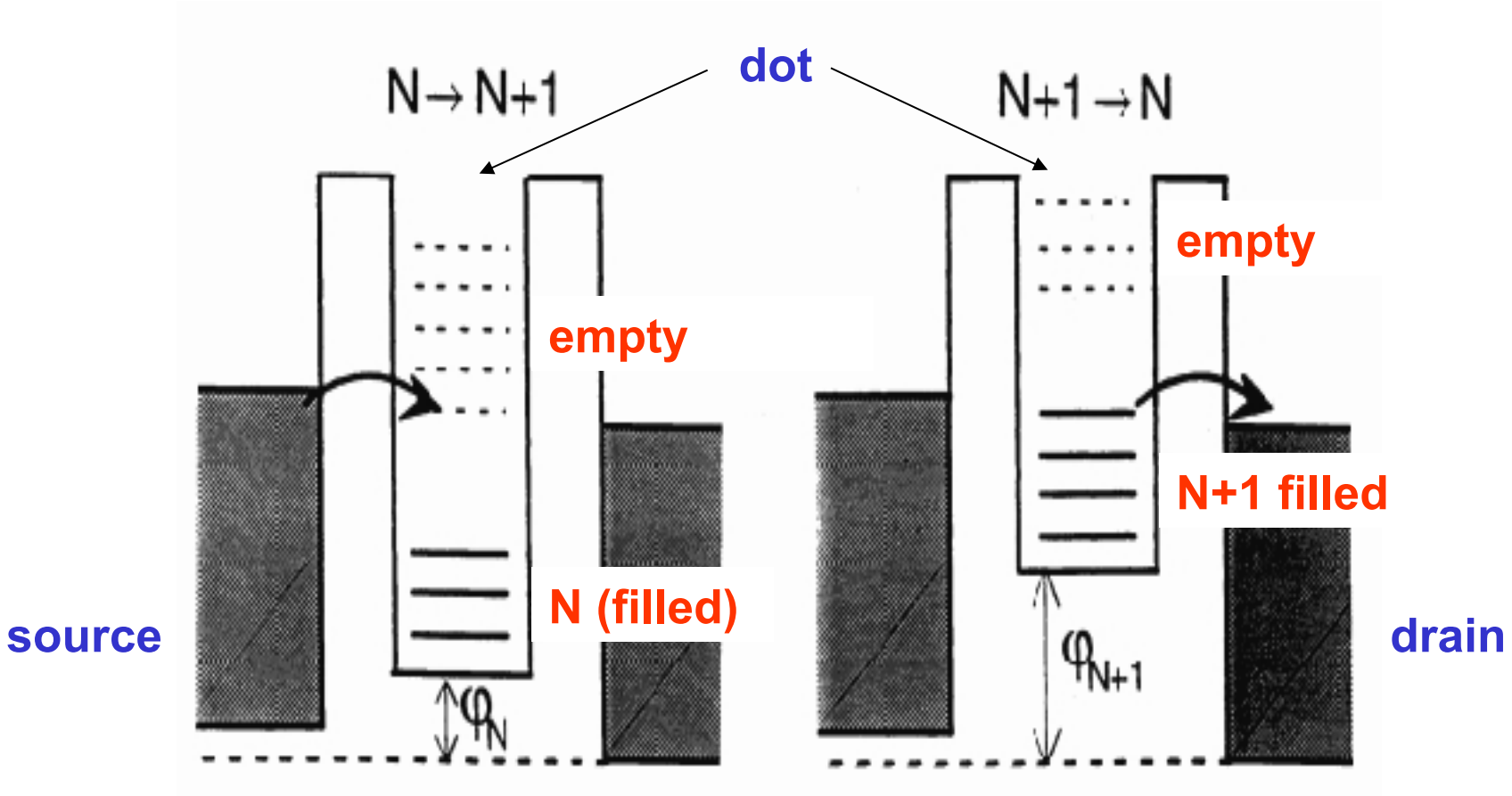

(For a detailed explanation see the annotation in the .ppt version.)

Charging a Dot, One Electron at a Time

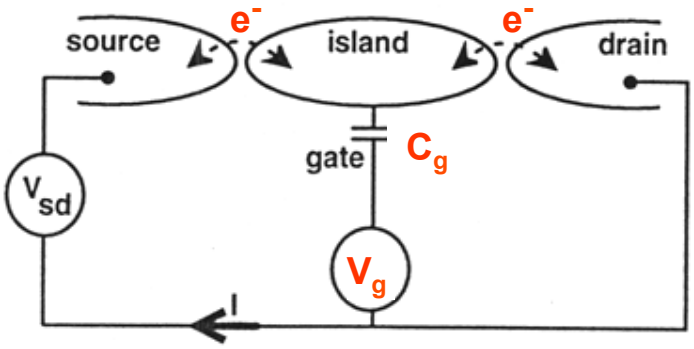

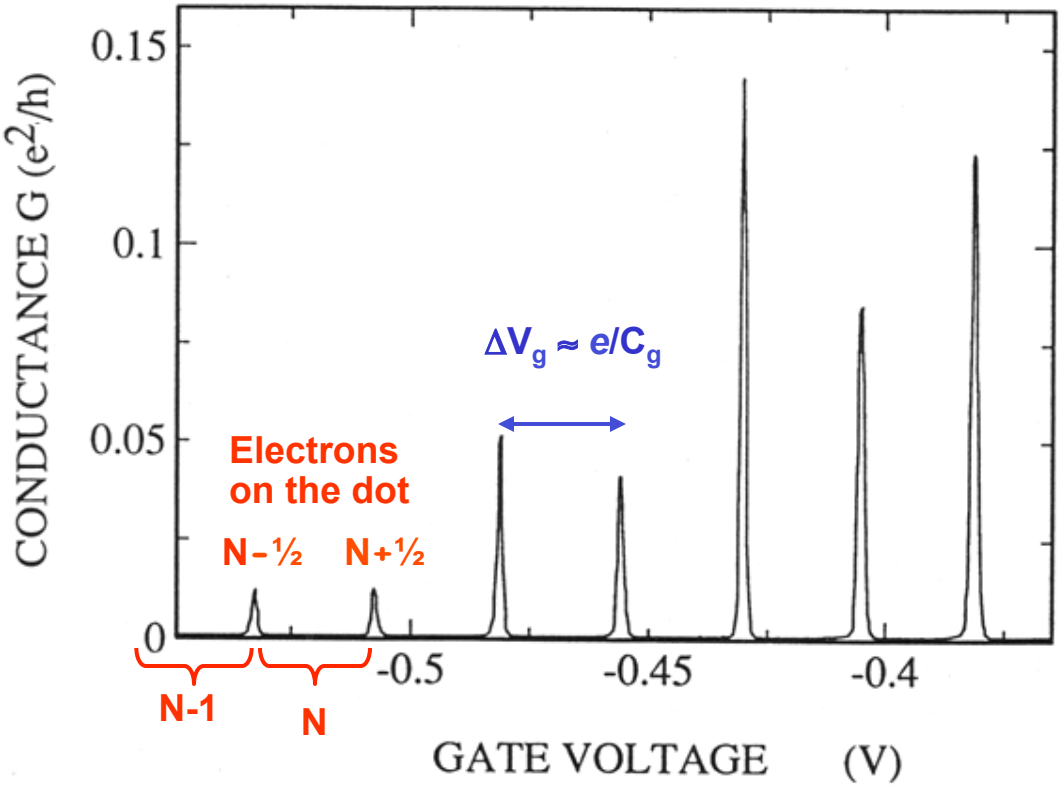

Sweeping the gate voltage V_g changes the charge Q_g on the gate-dot capacitor C_g. To add one electron requires the voltage $\Delta V_g \approx e/C_g$ since $C_g = Q_g/V_g$.

The source-drain conductance G is zero for most gate voltages, because putting even one extra electron onto the dot would cost too much Coulomb energy. This is called Coulomb blockade.

Electrons can hop onto the dot only at a gate voltage where the number of electrons on the dot flip-flops between N and N+1. Their time-averaged number is N+½ in that case.

The spacing between these half-integer conductance peaks is an integer.

The SET as Extremely Sensitive Charge Detector

At low temperature, the conductance peaks in a SET become very sharp.

Consequently, a very small change in the gate voltage half-way up a peak produces a large current change, i.e. a large amplification. That makes the SET extremely sensitive to tiny charges.

The flip side of this sensitivity is that a SET detects every nearby electron. When it hops from one trap to another, the SET produces a noise peak.

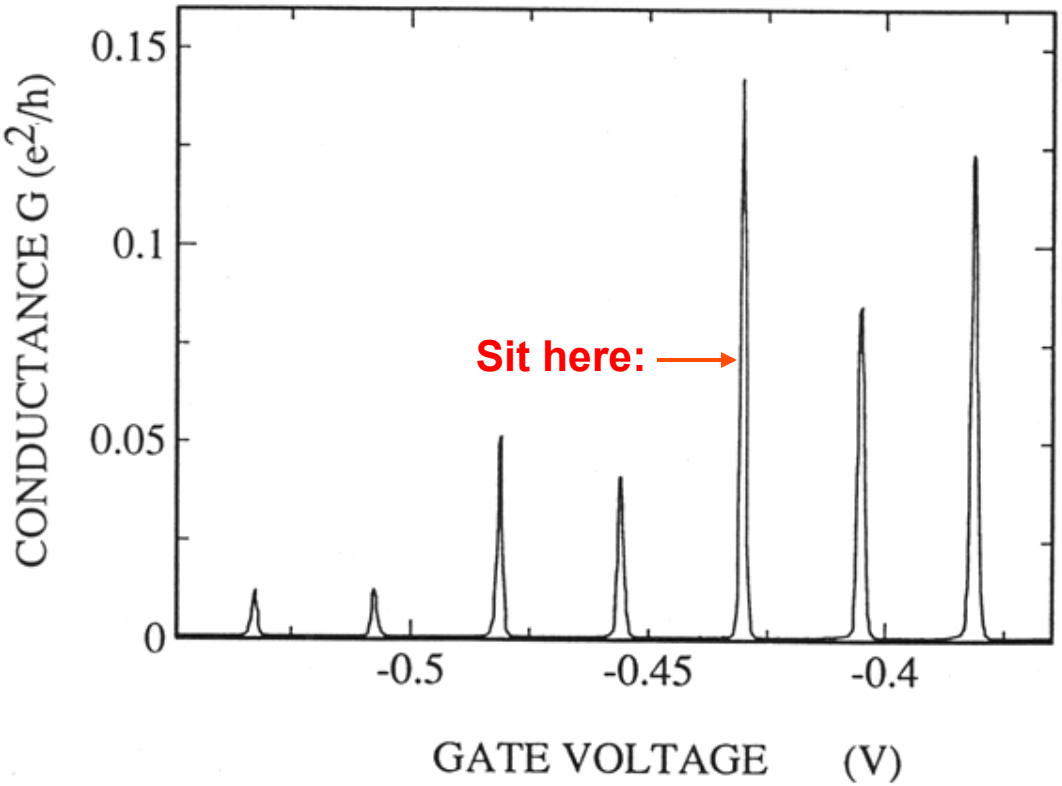

Gate Voltage versus Source-Drain Voltage

The situation gets a bit confusing, because there are two voltages that can be varied, the gate voltage V_g and the source-drain voltage $V_{s\text{-}d}$.

Both affect the conductance. Therefore, one often plots the conductance G against both voltages (see the next slide for data).

Schematically, one obtains "Coulomb diamonds", which are regions with a stable electron number N on the dot (and consequently zero conductance).

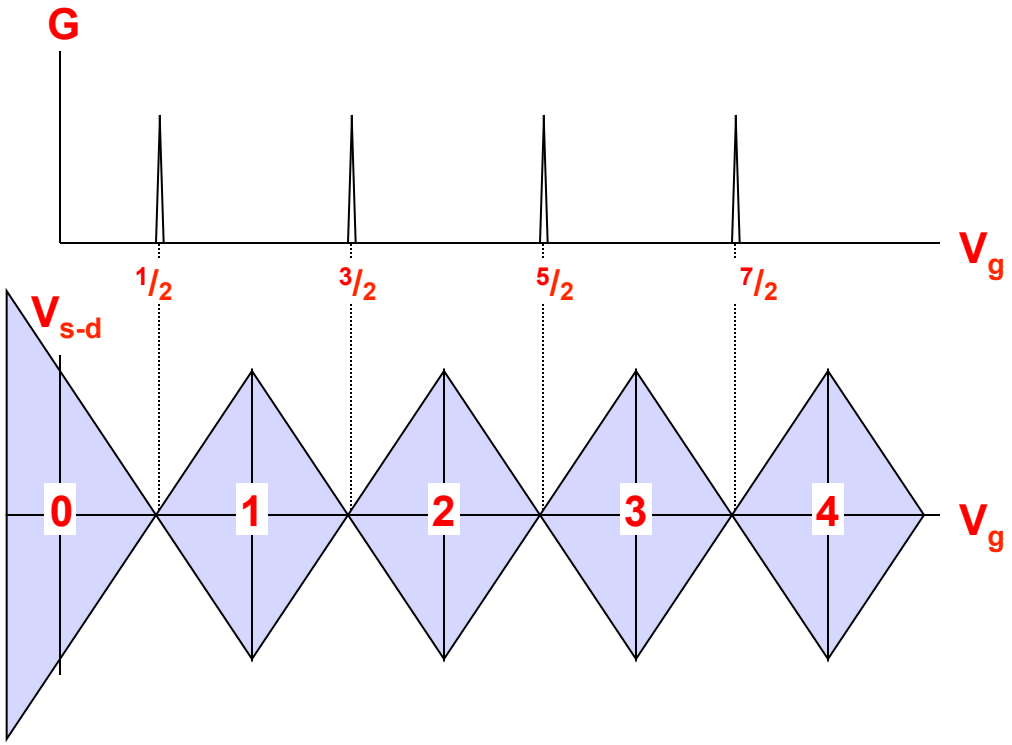

Gate Voltage (V)
-2.1
-1.0
Source-Drain Voltage (mV)
-10
0
10
Coulomb Diamonds
0=N
2
6
12
ΔVs
ΔVsd

Including the Energy Levels of a Quantum Dot

Contrary to the Coulomb blockade model, the data show Coulomb diamonds with uneven size. Some electron numbers have particularly large diamonds, indicating that the corresponding electron number is particularly stable.

This is reminiscent of the closed electron shells in atoms. Small dots behave like artificial atoms when their size shrinks down to the electron wavelength.

Continuous energy bands become quantized (see Lecture 8). Adding one electron requires the Coulomb energy U plus the difference ΔE between two quantum levels (next slide). If a second electron is added to the same quantum level (the same shell in an atom), ΔE vanishes and only the Coulomb energy U is needed.

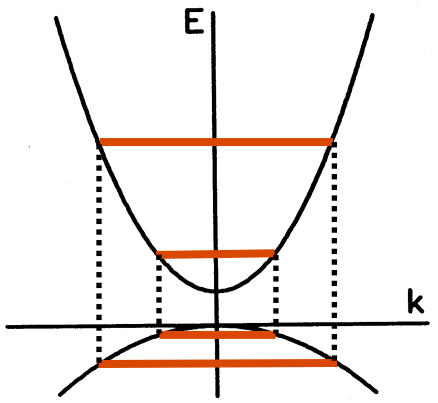

The quantum energy levels can be extracted from the spacing between the conductance peaks by subtracting the Coulomb energy $U = e^2/C$.

Quantum Dot in 2D (Disk)

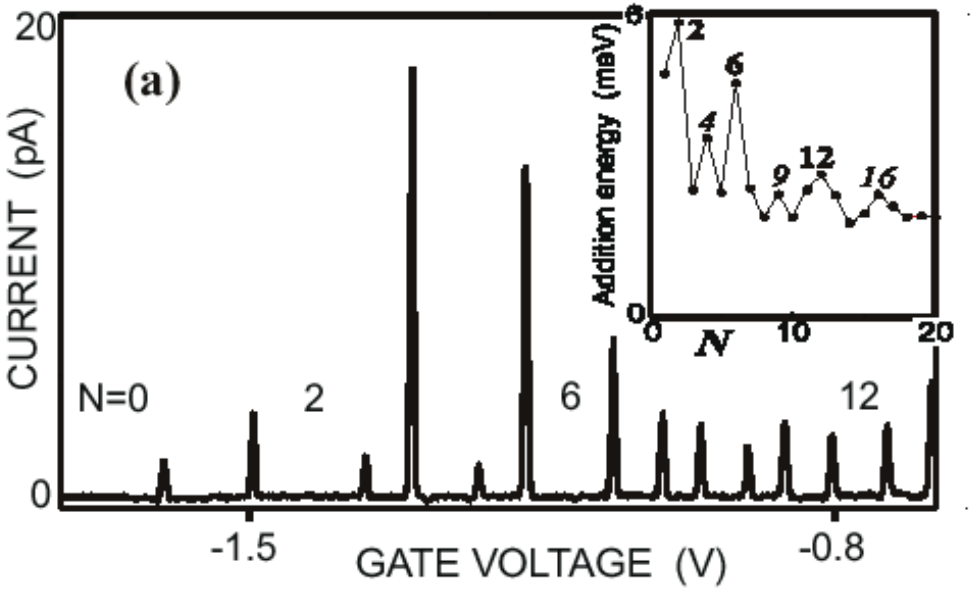

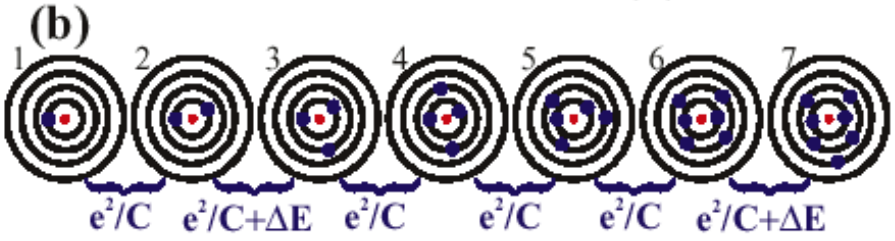

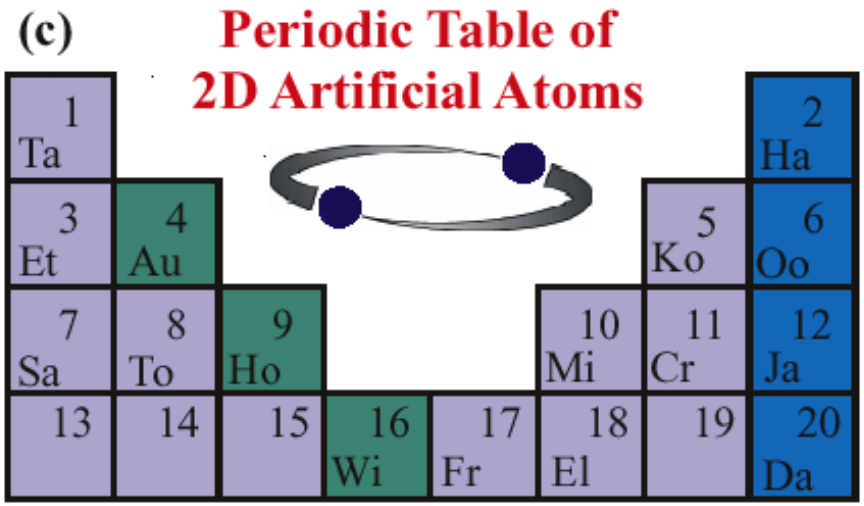

Filling the Electron Shells in 2D

Figure 2. Current flowing through a 2D circular quantum dot when varying the gate voltage. (a) The first peak marks the voltage where the 1st electron enters the dot, and the number of electrons, *N*, increases by one at each subsequent peak. The distance between adjacent peaks corresponds to the addition energies (see inset). (b) The addition of electrons to circular orbits is shown schematically. The first shell can hold 2 electrons whereas the second shell can contain up to 4 electrons. It therefore costs extra energy to add the 3rd and 7th electron. (c) The electronic properties following from a 2D shell structure can be summarized in a periodic table for 2 D elements. (The elements are named after team members from NTT and Delft.)

Shell Structure of Energy Levels for Various Potentials

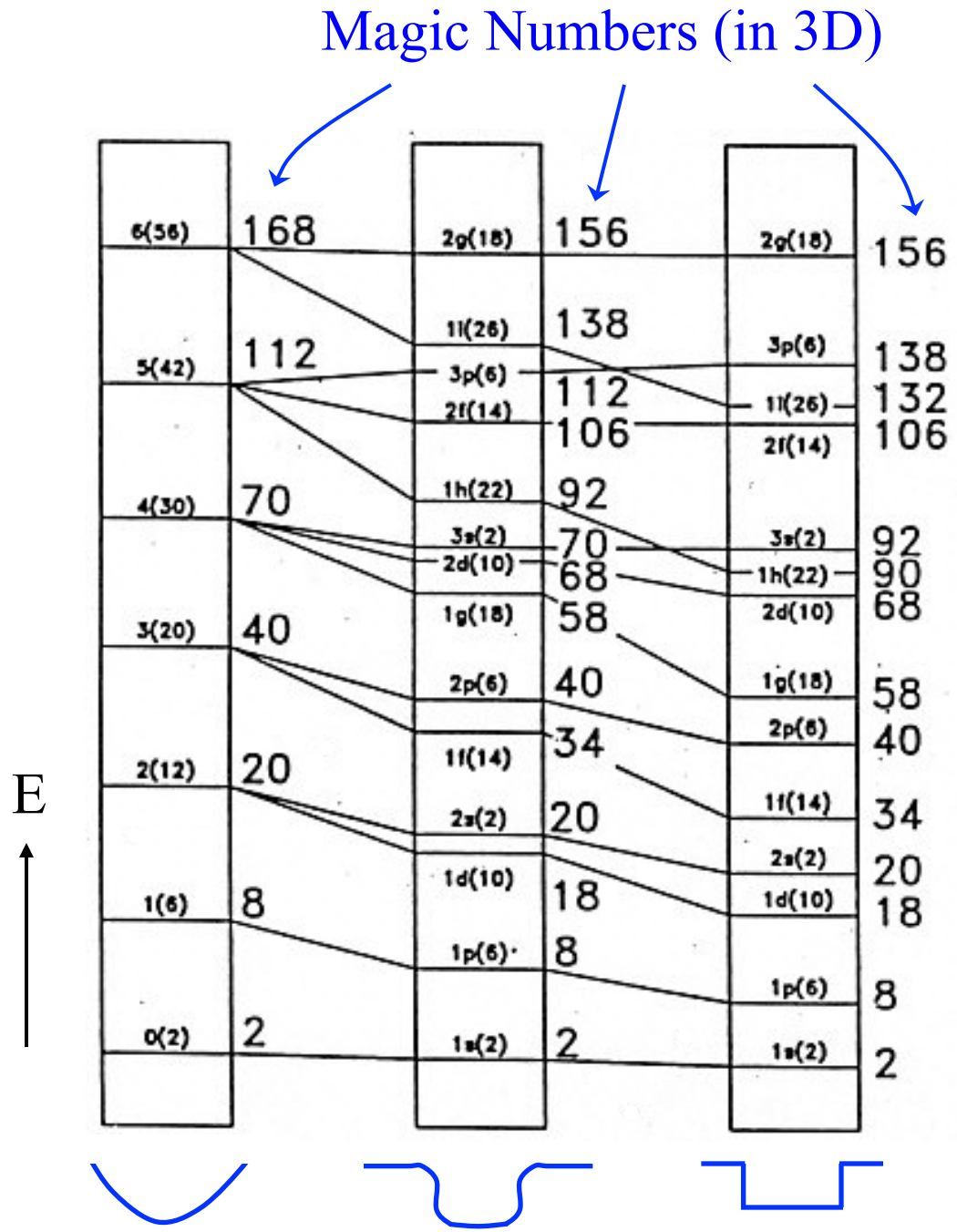

Precision Standards from “Single” Electronics

Count individual electrons, pairs, flux quanta

Current I
Coulomb
Blockade

$I = e\,f$

Voltage V
Josephson
Effect

$V = h/2e \cdot f$

$V/I = R = h/e^2$

Resistance R
Quantum
Hall Effect

(f = frequency)

Quantum interference

$$g = \sum_{m,n} |t_{nm}|^2$$

$$= \sum_{m,n} \sum_{\alpha} |t_{nm,\alpha}|^2 + \sum_{m,n} \sum_{\alpha \neq \beta} t_{nm,\alpha} (t_{nm,\beta})^*$$

$$= g_{\text{class}} + \delta g$$

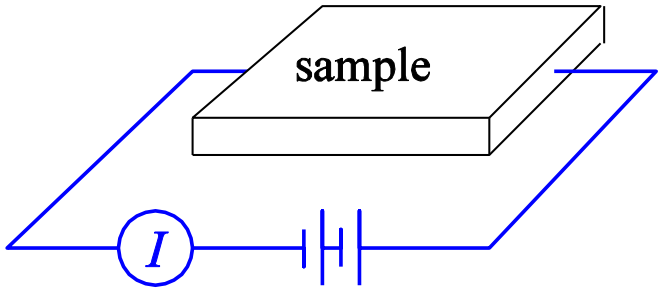

In general: δg small, random sign

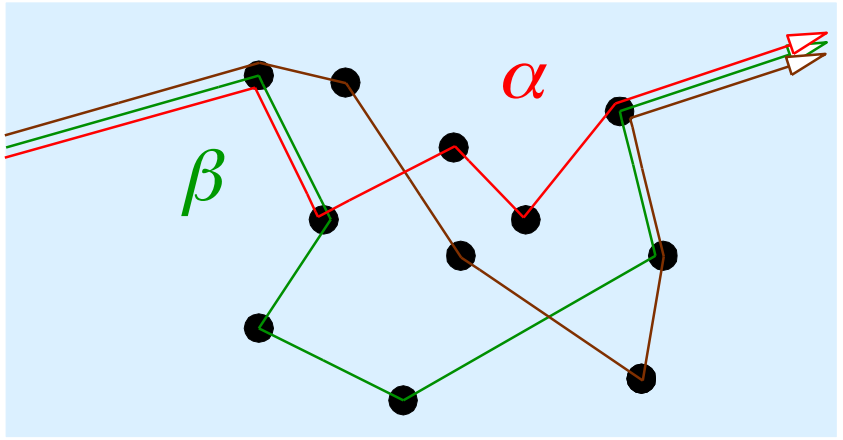

$t_{nm,\alpha}$, $t_{nm,\beta}$: amplitude for transmission along paths α, β

Quantum interference

$$g = \sum_{m,n} |t_{nm}|^2$$

$$= \boxed{\sum_{m,n} \sum_{\alpha} |t_{nm,\alpha}|^2} + \boxed{\sum_{m,n} \sum_{\alpha \neq \beta} t_{nm,\alpha} (t_{nm,\beta})^*}$$

$$= g_{\text{class}} + \delta g$$

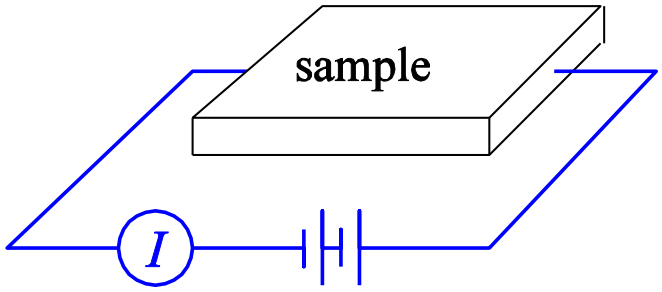

Three prototypical examples:

- Disordered wire
- Disordered quantum dot
- Ballistic quantum dot

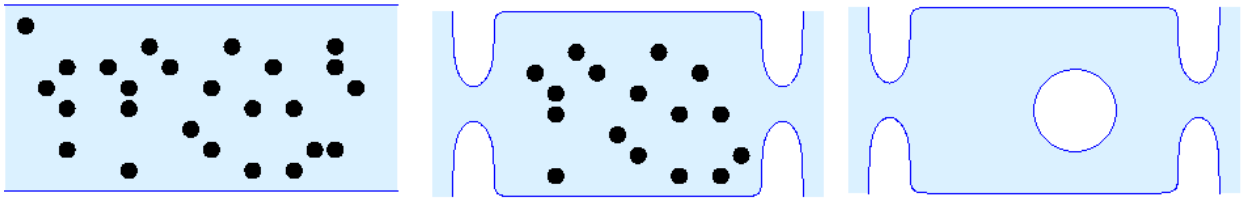

Scattering matrix and Green function

Recall: retarded Green function is solution of

$$(\varepsilon - \mathcal{H})\mathcal{G}^{\mathrm{R}}(\mathbf{r},\mathbf{r}';\omega) = \delta(\mathbf{r}-\mathbf{r}'),$$

In one dimension:

$$\mathcal{G}^{\mathrm{R}}(x,x';\varepsilon) = -\frac{i}{\hbar v} e^{ik|x-x'|},$$

$\varepsilon_k = \varepsilon$ and $v = \hbar^{-1}\mathrm{d}\varepsilon_k/\mathrm{d}k$

Green function in channel basis:

$$\mathcal{G}^{\mathrm{R}}(\mathbf{r},\mathbf{r}';\varepsilon) = \sum_{m=1}^{N_j}\sum_{n=1}^{N_k} \mathcal{G}^{\mathrm{R}}_{m,j;n,k}(x,x';\varepsilon)\chi_{m,j}(y)\chi_{n,k}(y').$$

r in lead j; ***r***’ in lead k

Substitute 1d form of Green function

$$\mathcal{G}^{\mathrm{R}}_{mn}(x,x') = -\frac{i}{\hbar v_m}\delta_{mn}\delta_{jk}e^{ik_m|x-x'|} - \frac{i}{\hbar(v_m v_n)^{1/2}} S_{m,j;n,k} e^{ik_m|x|+ik_n|x'|}.$$

If $j \neq k$:

$$\begin{aligned} S_{m,j;n,k} &= i\hbar(v_m v_n)^{1/2}\mathcal{G}^{\mathrm{R}}_{m,k;n,k}(0,0,\varepsilon) \\ &= i\hbar(v_m v_n)^{1/2}\int dy \int dy' \chi_{m,j}(y)\chi_{n,k}(y')\mathcal{G}^{\mathrm{R}}(\mathbf{r},\mathbf{r}';\varepsilon) \end{aligned}$$

Aharonov-Bohm (A-B) Effect

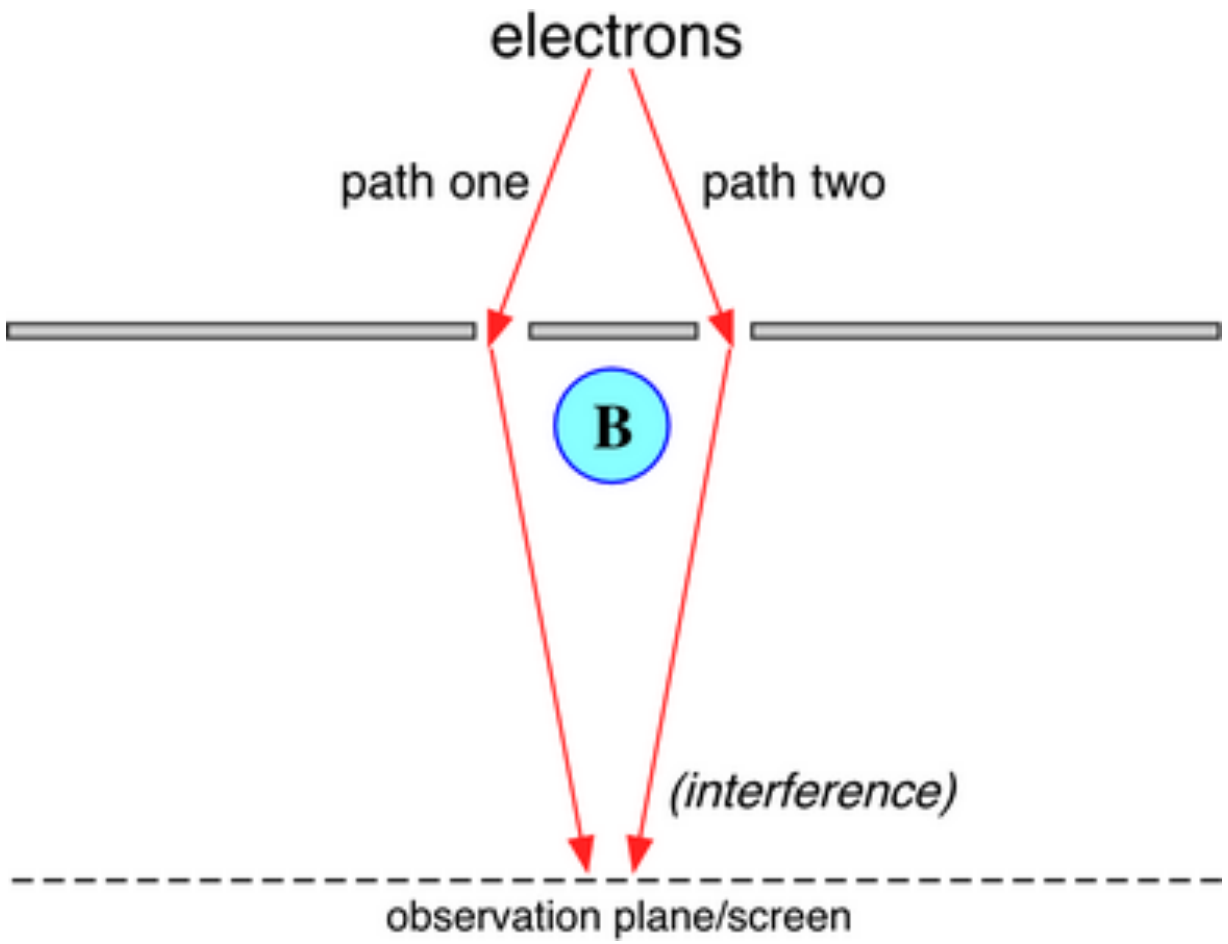

Illustration of interference experiment for Aharonov-Bohm effect

A-B Effect

- Comparison of non-B and B simulations

$$B = 0 = \nabla \times A \qquad \nabla \times A = B$$

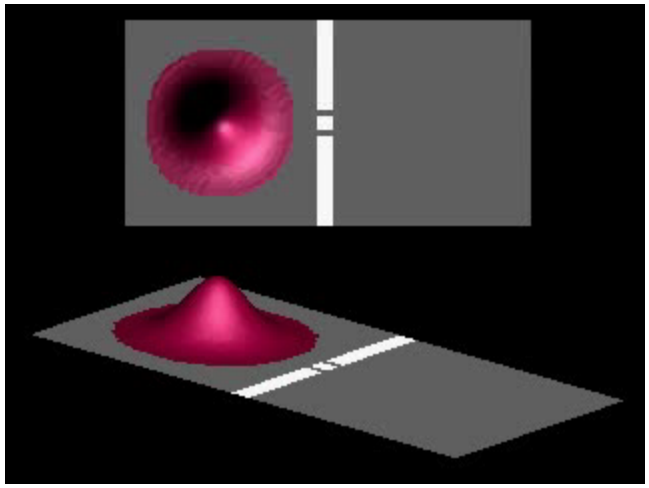

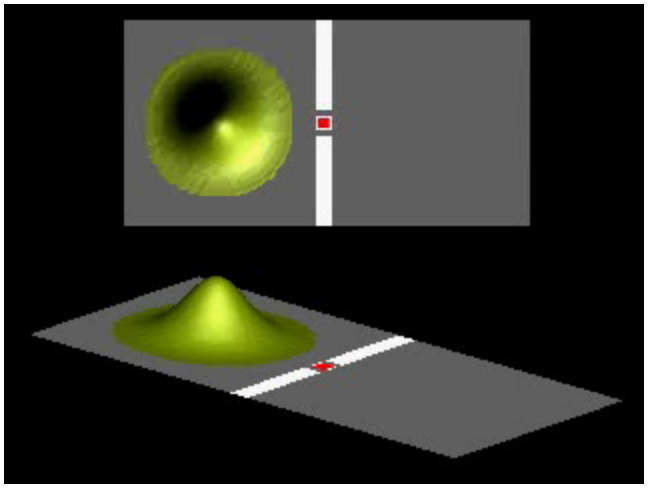

A-B Effect

- Formulations

$$\phi = \frac{q}{\hbar}\int_P A \cdot dx$$

$$\Delta\phi = \frac{q\Phi}{\hbar} \quad \text{(Magnetic A-B Effect)}$$

$$\Delta\phi = -\frac{qVt}{\hbar} \quad \text{(Electric A-B Effect)}$$

Ring Oscillations

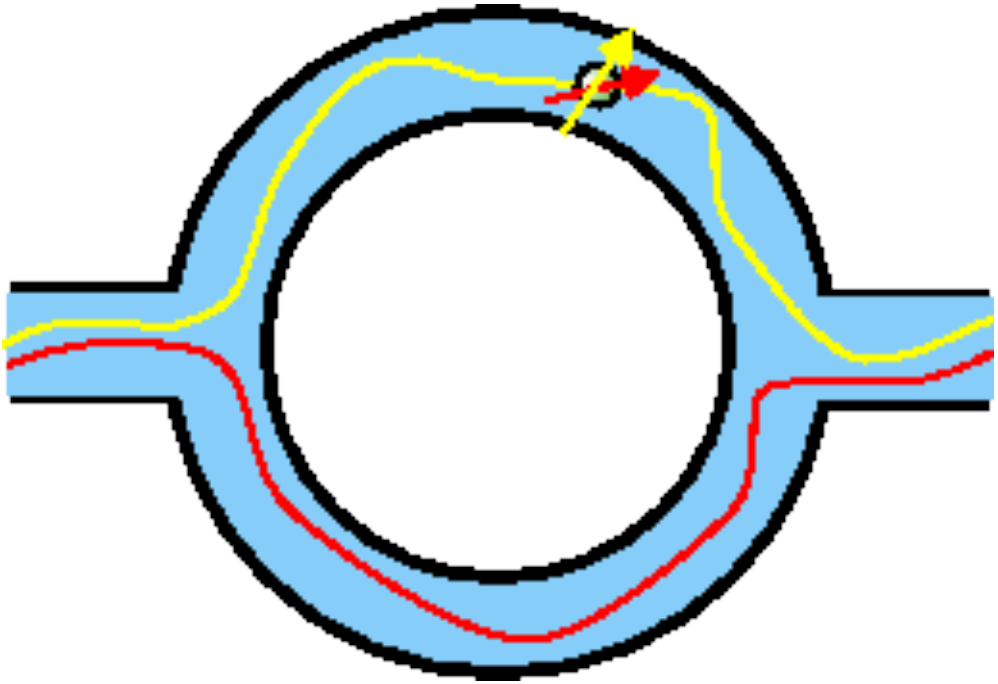

Ring Oscillation without E/B Field

Ring Oscillations

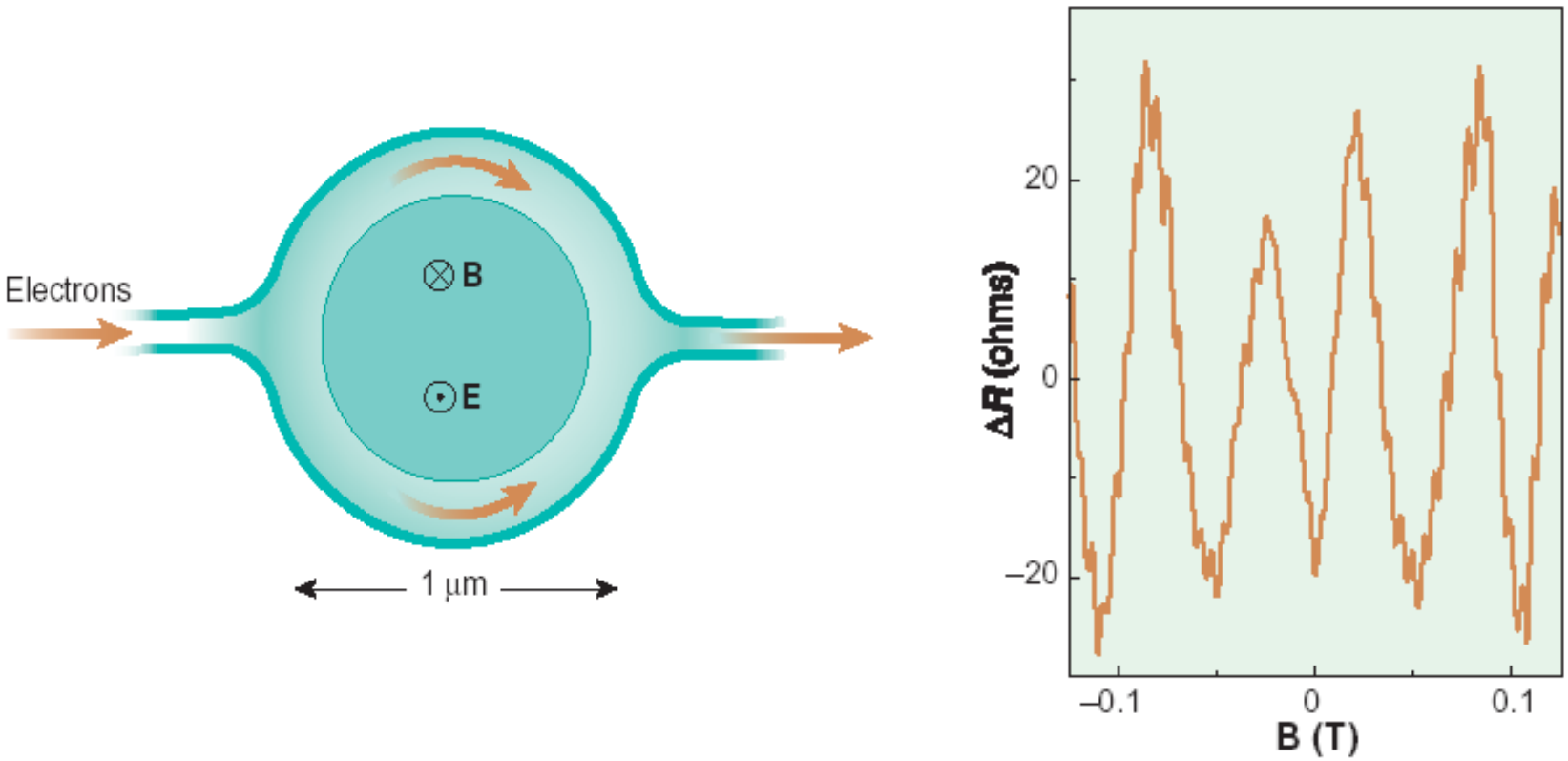

Ring Oscillations with E/B Field

Ring Oscillation

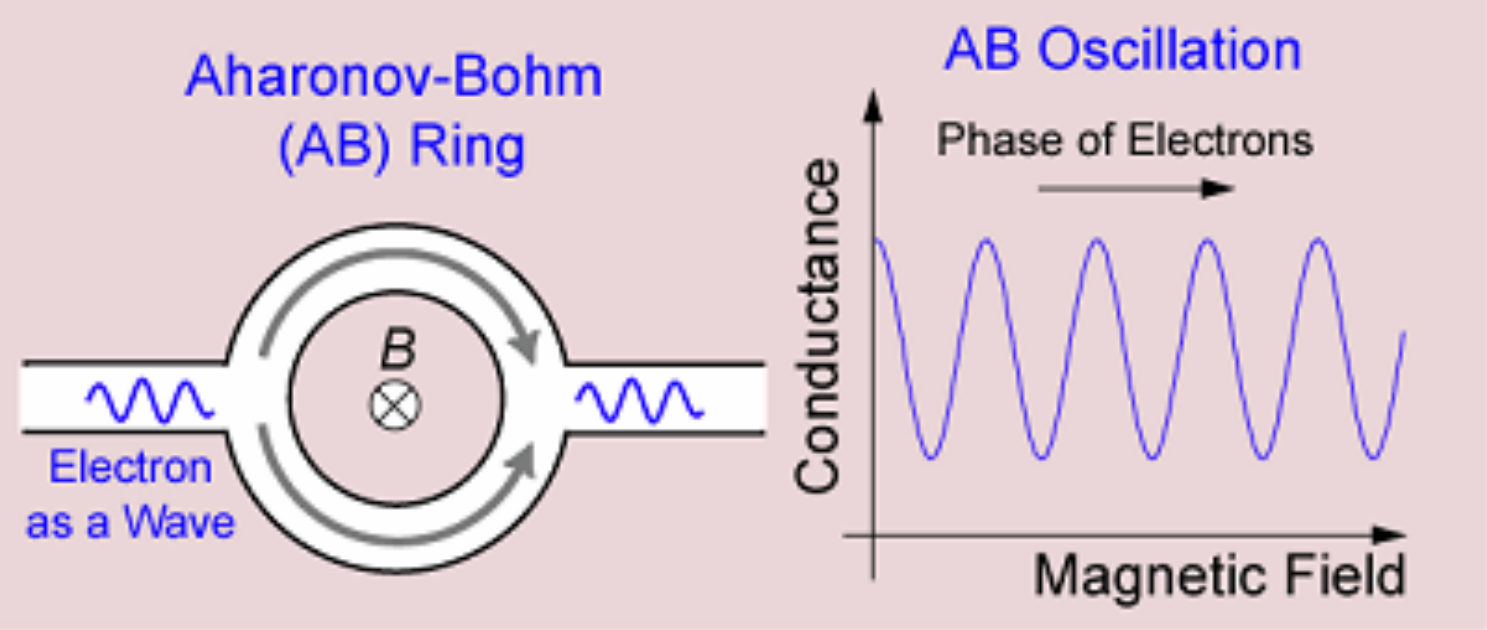

$$\Delta R = \frac{\pi r^2 B}{NWt2e}$$

A-B Ring Applications

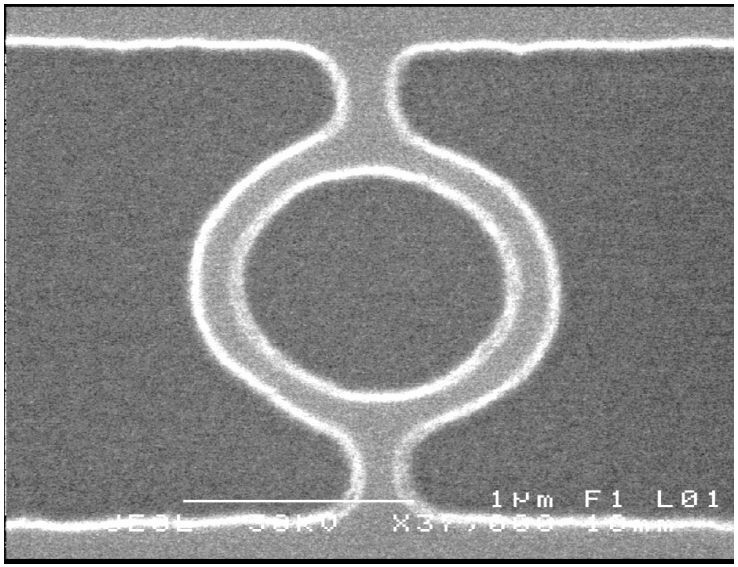

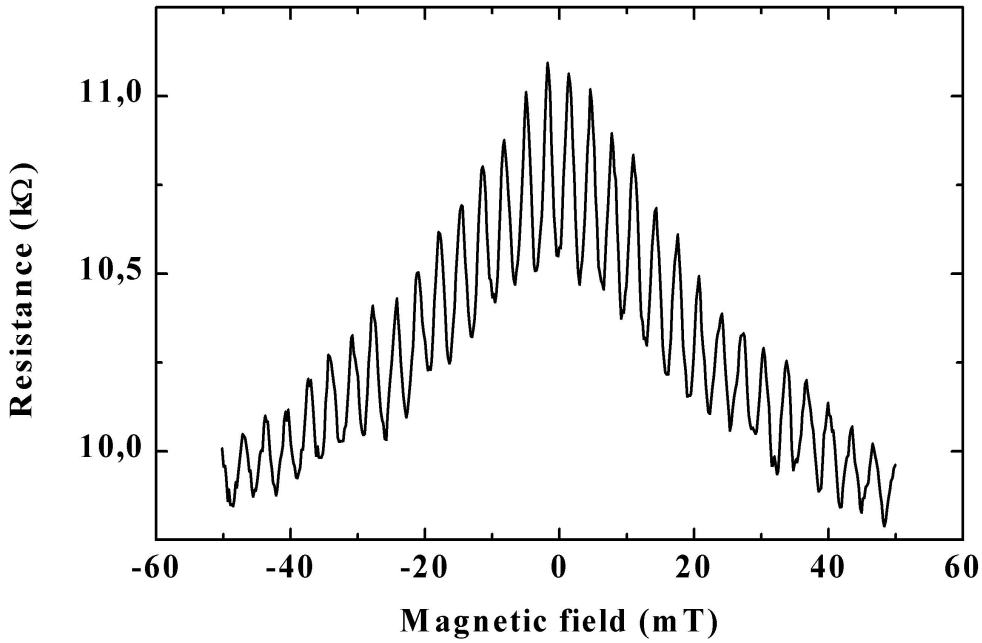

A-B Ring in Semiconductor

A-B Ring Applications

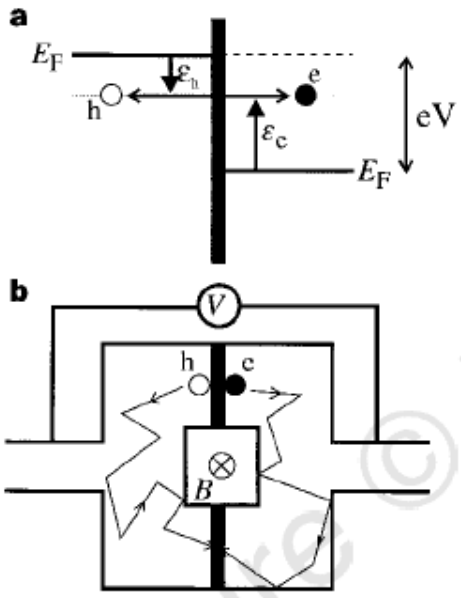

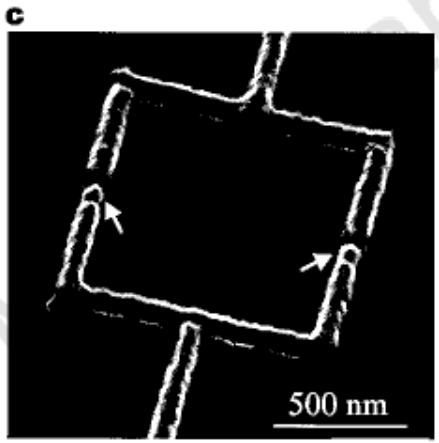

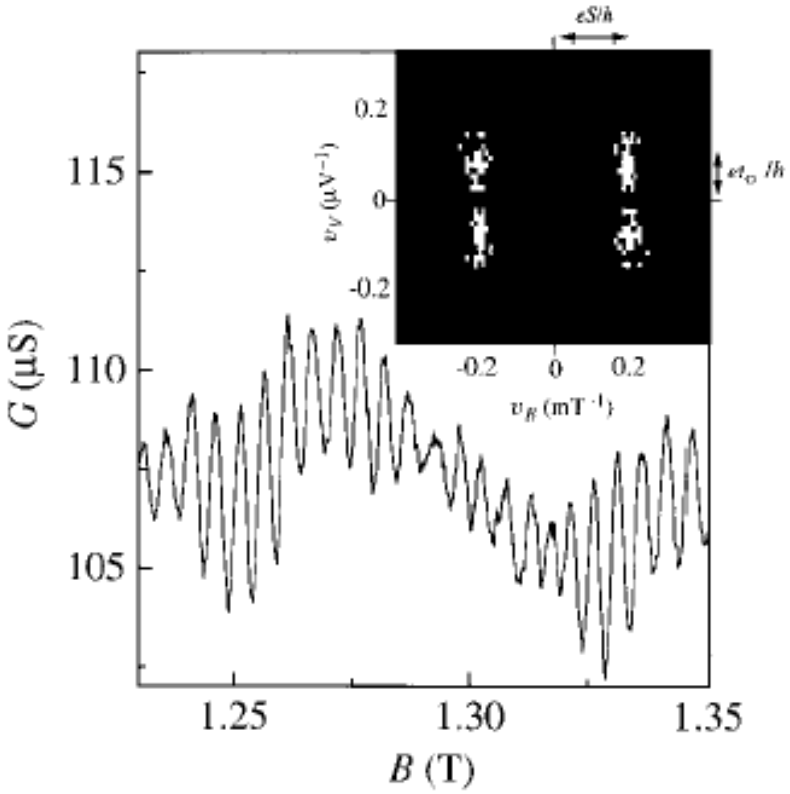

A-B Ring in Metal

A-B Ring Applications

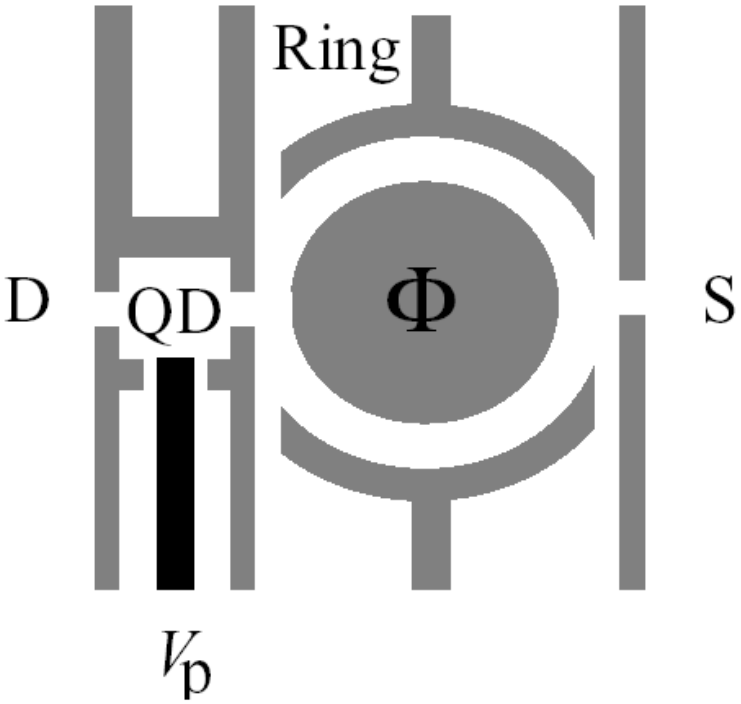

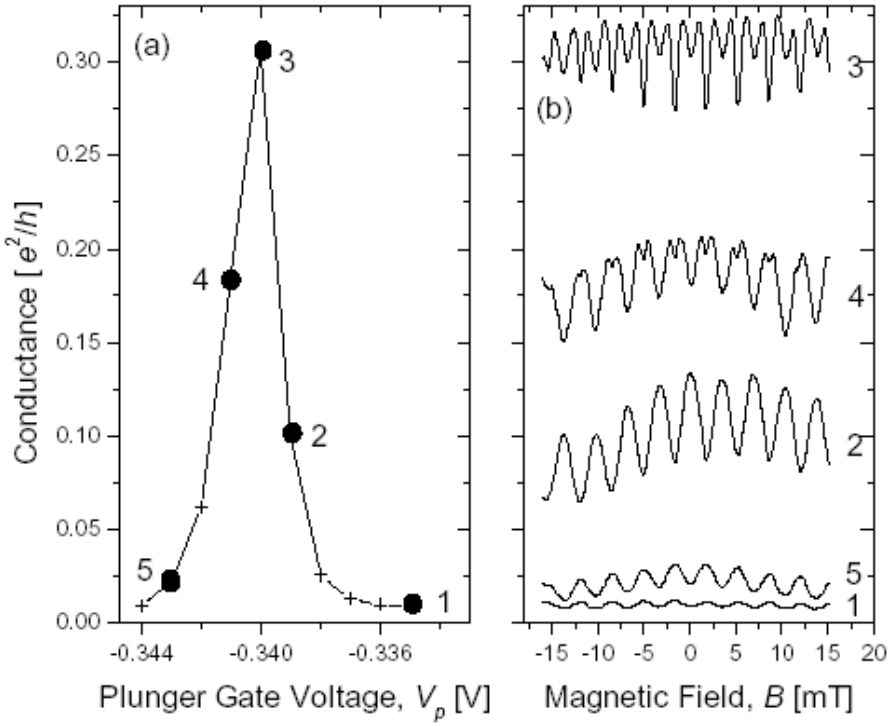

A-B oscillation in a Ring with a QD connected in series

A-B Ring Applications

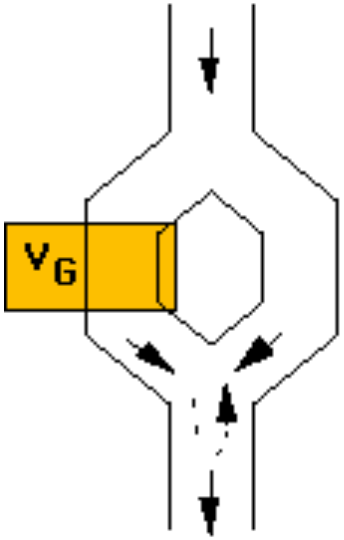

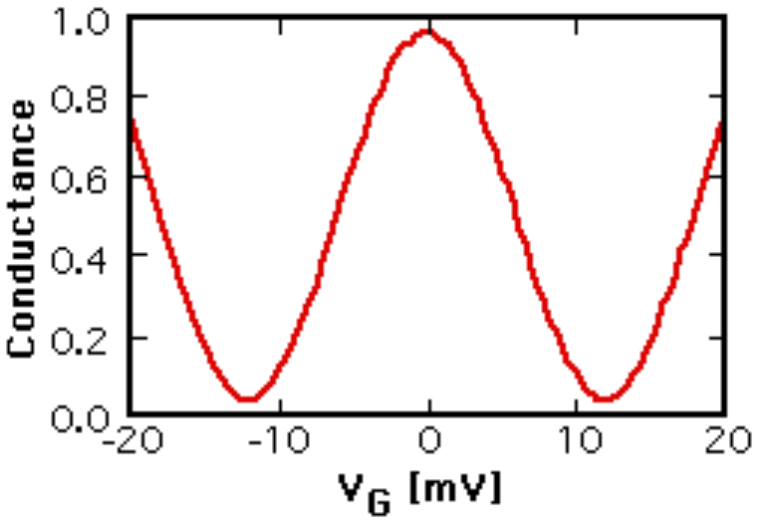

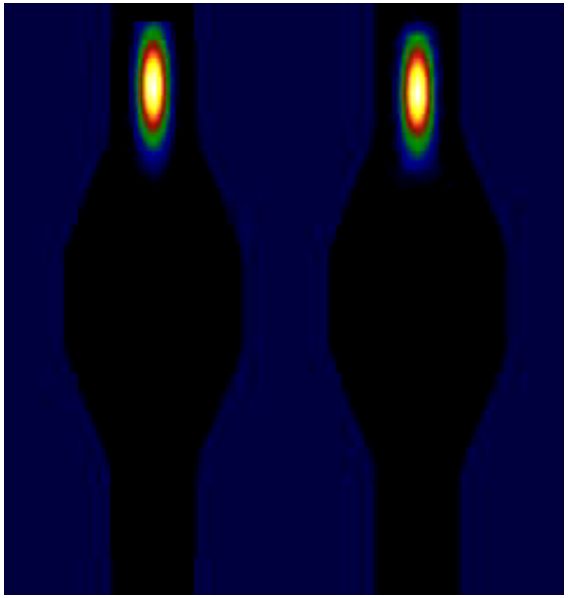

A-B interferometer